AFRL-PR-WP-TM-2006-2131

EXPERIMENTAL AND COMPUTATIONAL CHARACTERIZATION OF COMBUSTION PHENOMENA

Dr. James R. Gord

Combustion Branch (AFRL/PRTC)
Turbine Engine Division
Propulsion Directorate
Air Force Materiel Command, Air Force Research Laboratory
Wright-Patterson Air Force Base, OH 45433-7251

MAY 2006

Final Report for 01 October 1996 – 01 May 2006

PROPULSION DIRECTORATE
AIR FORCE MATERIEL COMMAND
AIR FORCE RESEARCH LABORATORY
WRIGHT-PATTERSON AIR FORCE BASE, OH 45433-7251

NOTICE

Using Government drawings, specifications, or other data included in this document for any purpose other than Government procurement does not in any way obligate the U.S. Government. The fact that the Government formulated or supplied the drawings, specifications, or other data does not license the holder or any other person or corporation; or convey any rights or permission to manufacture, use, or sell any patented invention that may relate to them.

This report was cleared for public release by the Air Force Research Laboratory Wright Site (AFRL/WS) Public Affairs Office (PAO) and is releasable to the National Technical Information Service (NTIS). It will be available to the general public, including foreign nationals.

PAO case number: AFRL-WS 06-1425
Date cleared: 2 Jun 06

THIS TECHNICAL REPORT IS APPROVED FOR PUBLICATION.

*//Signature//

JAMES R. GORD, PhD
Project Monitor
Combustion Branch

//Signature//

ROBERT D. HANCOCK, PhD
Chief
Combustion Branch

//Signature//

WILLIAM W. COPENHAVER
Acting Chief Engineer
Turbine Engine Division
Propulsion Directorate

This report is published in the interest of scientific and technical information exchange and its publication does not constitute the Government's approval or disapproval of its ideas or findings.

*Disseminated copies will show "//Signature//" stamped or typed above the signature blocks.

REPORT DOCUMENTATION PAGE

Form Approved
OMB No. 0704-0188

1. REPORT DATE *(DD-MM-YY)*	2. REPORT TYPE	3. DATES COVERED *(From - To)*
May 2006	Final	10/01/1996 – 05/01/2006

4. TITLE AND SUBTITLE
EXPERIMENTAL AND COMPUTATIONAL CHARACTERIZATION OF COMBUSTION PHENOMENA

5a. CONTRACT NUMBER
In-house

5b. GRANT NUMBER

5c. PROGRAM ELEMENT NUMBER
61102F

6. AUTHOR(S)
Dr. James R. Gord

5d. PROJECT NUMBER
2308

5e. TASK NUMBER
P7

5f. WORK UNIT NUMBER
01

7. PERFORMING ORGANIZATION NAME(S) AND ADDRESS(ES)

Combustion Branch (AFRL/PRTC)
Turbine Engine Division
Propulsion Directorate
Air Force Materiel Command, Air Force Research Laboratory
Wright-Patterson Air Force Base, OH 45433-7251

8. PERFORMING ORGANIZATION REPORT NUMBER
AFRL-PR-WP-TR-2006-2131

9. SPONSORING/MONITORING AGENCY NAME(S) AND ADDRESS(ES)

Propulsion Directorate
Air Force Research Laboratory
Air Force Materiel Command
Wright-Patterson AFB, OH 45433-7251

10. SPONSORING/MONITORING AGENCY ACRONYM(S)
AFRL-PR-WP

11. SPONSORING/MONITORING AGENCY REPORT NUMBER(S)
AFRL-PR-WP-TR-2006-2131

12. DISTRIBUTION/AVAILABILITY STATEMENT
Approved for public release; distribution is unlimited.

13. SUPPLEMENTARY NOTES
Report contains color.

PAO case number: AFRL/WS 06-1425; Date cleared: 02 Jun 2006.

14. ABSTRACT
Propulsion systems represent a substantial fraction of the cost, weight, and complexity of Air Force aircraft, spacecraft, and other weapon-system platforms. The vast majority of these propulsion systems are powered through combustion of fuel; therefore, the detailed study of combustion has emerged as a highly relevant and important field of endeavor. Much of the work performed by today's combustion scientists and engineers is devoted to the tasks of improving propulsion-system performance while simultaneously reducing pollutant emissions. Increasing the affordability, maintainability, and reliability of these critical propulsion systems is a major driver of activity as well. This research effort is designed to forward the scientific investigation of combustion phenomena through an integrated program of fundamental combustion studies, both experimental and computational, supported by parallel efforts to develop, demonstrate, and apply advanced techniques in laser-based/optical diagnostics and modeling and simulation.

15. SUBJECT TERMS
Combustion, Flames, Turbulence, Diagnostics, Measurements, Lasers, Optics, Modeling, Simulation, Computational Fluid Dynamics

16. SECURITY CLASSIFICATION OF:			17. LIMITATION OF ABSTRACT:	18. NUMBER OF PAGES	19a. NAME OF RESPONSIBLE PERSON (Monitor)
a. REPORT	b. ABSTRACT	c. THIS PAGE			Dr. James R. Gord
Unclassified	Unclassified	Unclassified	SAR	64	19b. TELEPHONE NUMBER *(Include Area Code)* N/A

Standard Form 298 (Rev. 8-98)
Prescribed by ANSI Std. Z39-18

Experimental and Computational Characterization of Combustion Phenomena

Abstract

Propulsion systems represent a substantial fraction of the cost, weight, and complexity of Air Force aircraft, spacecraft, and other weapon-system platforms. The vast majority of these propulsion systems are powered through combustion of fuel; therefore, the detailed study of combustion has emerged as a highly relevant and important field of endeavor. Much of the work performed by today's combustion scientists and engineers is devoted to the tasks of improving propulsion-system performance while simultaneously reducing pollutant emissions. Increasing the affordability, maintainability, and reliability of these critical propulsion systems is a major driver of activity as well. This research effort is designed to forward the scientific investigation of combustion phenomena through an integrated program of fundamental combustion studies, both experimental and computational, supported by parallel efforts to develop, demonstrate, and apply advanced techniques in laser-based/optical diagnostics and modeling and simulation.

Introduction

This final report comprises six previously released documents describing efforts conducted during this Air Force Office of Scientific Research-funded in-house research and development program. The first four documents are four-page abstracts prepared in conjunction with the Air Force Office of Scientific Research/Army Research Office Contractors Meeting on Chemical Propulsion for FY06, FY05, FY04, and FY03, respectively. The fifth document is an invited paper entitled "Emerging Combustion Diagnostics" presented in January 2001 at the 39th American Institute of Aeronautics and Astronautics Aerospace Sciences Meeting and Exhibit in Reno NV. This paper describes a number of fundamental diagnostics-development efforts predating those covered in the contractors-meeting abstracts. The sixth and final document is an invited paper entitled "Optical Turbine-Engine Diagnostics for Ground-Test and On-Board Applications" prepared for the NATO Research & Technology Agency Applied Vehicle Technology Panel Specialists Meeting on Recent Developments in Non-Intrusive Measurement Technology for Military Application on Model and Full-Scale Vehicles (AVT-124), which was held during April 2005 in Budapest, Hungary. This paper documents practical applications of numerous optical measurement techniques developed during this in-house research and development program. Together these six documents constitute a representative overview of the work accomplished through this program.

Abstract for FY06 AFOSR/ARO Contractors Meeting on Chemical Propulsion

EXPERIMENTAL AND COMPUTATIONAL CHARACTERIZATION OF COMBUSTION PHENOMENA

AFOSR Task No. 02PR01COR

Principal Investigator: James R. Gord

Air Force Research Laboratory
AFRL/PRTC Bldg 5
1950 Fifth St
Wright-Patterson AFB OH 45433-7251

SUMMARY/OVERVIEW

Propulsion systems represent a substantial fraction of the cost, weight, and complexity of Air Force aircraft, spacecraft, and other weapon-system platforms. The vast majority of these propulsion systems are powered through combustion of fuel; therefore, the detailed study of combustion has emerged as a highly relevant and important field of endeavor. Much of the work performed by today's combustion scientists and engineers is devoted to the tasks of improving propulsion-system performance while simultaneously reducing pollutant emissions. Increasing the affordability, maintainability, and reliability of these critical propulsion systems is a major driver of activity as well. This research effort is designed to forward the scientific investigation of combustion phenomena through an integrated program of fundamental combustion studies, both experimental and computational, supported by parallel efforts to develop, demonstrate, and apply advanced techniques in laser-based/optical diagnostics and modeling and simulation.

TECHNICAL DISCUSSION

Extension of Diode-Laser-Based Sum- and Difference-Frequency Generation to Two-Line Thermometry and Wavelength-Modulation Spectroscopy. Compact, high-speed-tunable, diode-laser-based ultraviolet (UV) and mid-infrared (MIR) laser sources have been developed to take advantage of strong electronic transitions and fundamental vibrational bands for *in-situ* combustion sensing. These sources are based on sum- and difference-frequency generation, respectively, and have been operated with data-acquisition bandwidths of 10 to 20 kHz. Measurements of species concentration and temperature have been achieved by resolving the lineshape of single transitions, although the accuracy of this approach can be limited by uncertainties in the collisional environment. In unsteady flames, for example, the concentration of various colliding species may not be known. In addition, collisional cross-sections may not be available for all conditions encountered in realistic combustors. To improve measurement accuracy over a wide range of conditions, we have implemented a two-line thermometric approach using both direct absorption and wavelength-modulation spectroscopy (WMS). WMS requires additional calibration procedures but offers improved sensitivity for low concentrations. Demonstration measurements are performed for various equivalence ratios in a H_2-air diffusion flame stabilized over a Hencken burner. Figure 1 shows a wavelength scan over two OH transitions, along with the corresponding WMS signal. Improved temperature accuracy is achieved by taking the ratio of the integrated absorption across two transitions, which reduces uncertainties associated with collisional broadening.

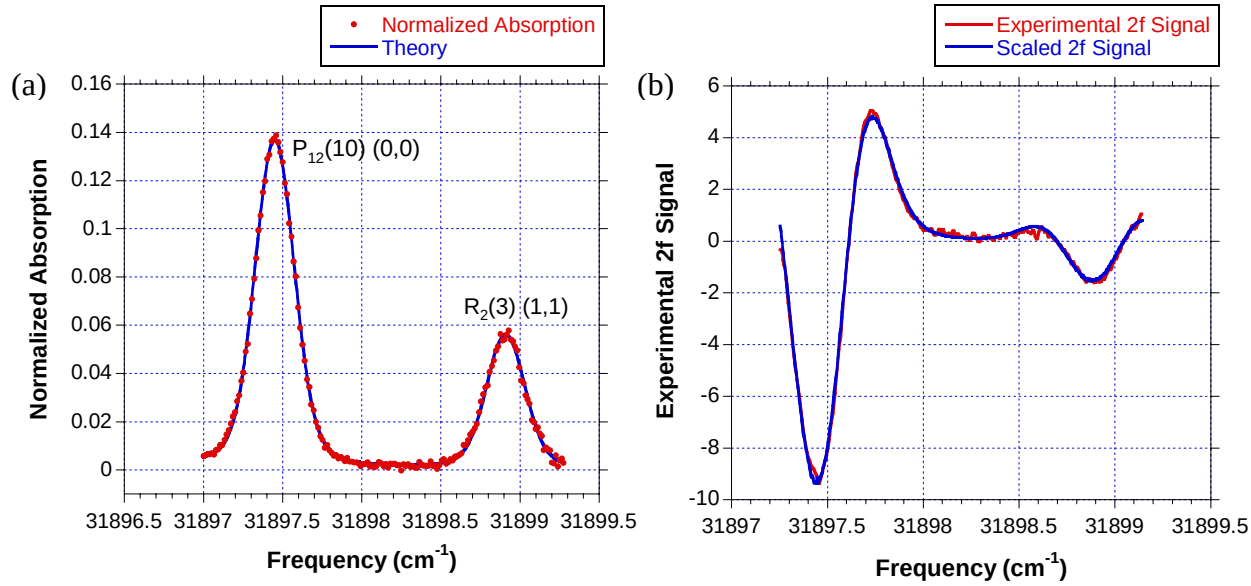

Fig. 1. Two-line OH spectra using (a) direct absorption and (b) wavelength-modulation spectroscopy.

Ultrafast Coherent Anti-Stokes Raman Scattering for Thermometry. Most previous CARS thermometric measurements in gas-phase or reacting flows have been performed using ns laser pulses. A major limitation of ns-laser-based CARS thermometry is the contribution of the nonresonant signal, which limits the accuracy and degrades the sensitivity of the technique. Moreover, most of these measurements are generally performed at low repetition rate (generally 10-20 Hz) due to the unavailability of high-rep-rate, high-power ns lasers. This temporal resolution complicates efforts to resolve turbulence phenomena in reacting flows.

In fs CARS, also known as FAST (Femtosecond Adaptive Spectroscopic Technique) CARS, a coherence is established in the medium by using two nearly transform-limited fs lasers whose frequency difference corresponds to the resonant frequencies of the excited molecule, covering the whole vibration-rotation manifold in the ground electronic state. On the order of one hundred fs after the initial excitation, the coherently excited transitions begin to dephase with respect to each other due to slight frequency differences between neighboring transitions, and the overall signal starts to decay. In our work, we focus on the initial decay of the coherence for extracting the temperature of the medium. The initial decay rate of the coherence is very sensitive to temperature and is not affected by collision rates or Stark shifts, two factors which significantly complicate frequency-domain nanosecond CARS measurements.

In general, there are four promising advantages of short-pulse CARS spectroscopy: (1) it improves accuracy by reducing or eliminating the non-resonant contribution to the CARS signal when the probe beam is delayed with respect to the pump beam, (2) it minimizes the effects of collisions on the CARS signal, thereby reducing modeling uncertainty and increasing signal-to-noise ratio, (3) it improves sensitivity and might enable the detection of minor species due to reduction or elimination of interference from the non-resonant background, and (4) it has the capability of generating signals at rates up to 1 kHz. These advantages have the potential to enhance the performance of CARS thermometry in high-pressure, high-temperature combustors of practical interest by overcoming known limitations of ns-based systems.

A schematic diagram of the fs CARS system at WPAFB and CARS signals obtained as a function of probe delay in atmospheric-pressure nitrogen with a nearly transform-limited, 50-fs probe beam are shown in Fig. 2 for three different temperatures. The CARS signals decrease sharply for probe delays from 0-4 ps through initial dephasing due to the frequency spread of the

rovibrational transitions in the fundamental Raman band. At 300 K, the fundamental band has a FWHM of approximately 4 cm^{-1}, corresponding to a characteristic decay time of approximately 3-4 psec. Following this initial decay, the CARS signal exhibits a long-lived beating pattern due to constructive and destructive interference of the Raman coherences. This long-lived beating pattern decays slowly through collisional dephasing. The 500 K signal decays much faster because the frequency spread of those Raman transitions with significant induced intensity is much greater at the higher temperature.

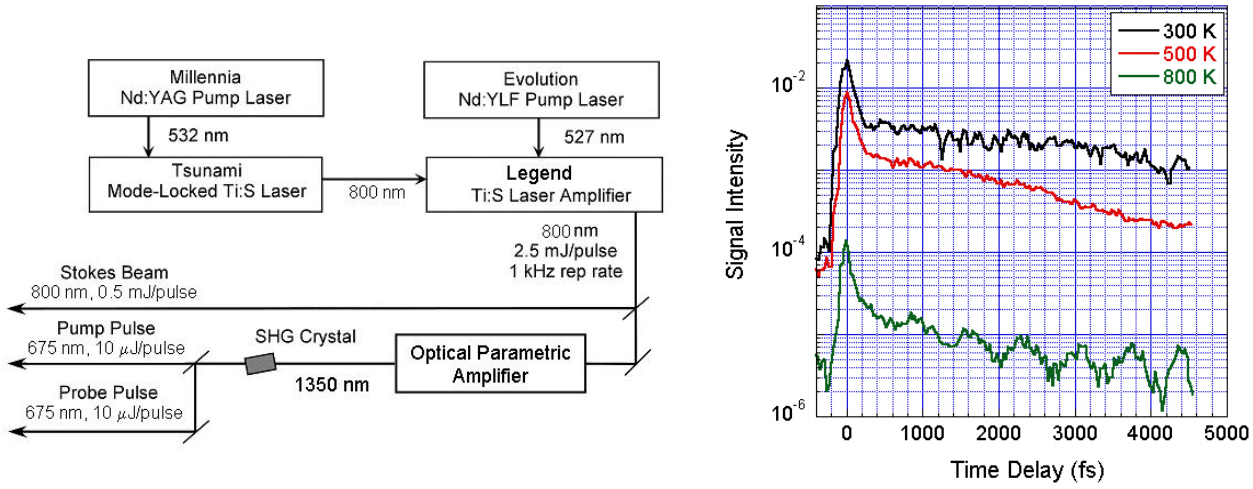

(a) (b)

Figure 2. (a) Schematic diagram of the fsec CARS system and (b) fsec CARS signal for three different temperatures for the temporal region near the pump/Stokes excitation.

Electronic-Resonance-Enhanced CARS for Detection of Nitric Oxide. Accurate measurement of NO concentration in high-pressure combustors is very difficult but critical for minimization of pollutant emissions. Current state-of-the-art measurements of NO concentration in high-pressure liquid-fueled combustors are based on laser-induced fluorescence (LIF), which has four major limitations: (1) significant quenching of the NO LIF signal by O_2, CO_2, H_2O, and other molecules, (2) decreasing NO LIF signal with increasing pressure for a given temperature and NO mole fraction, (3) interferences from soot luminescence typical of complex jet fuels, and (4) absorption of the laser beam and LIF signal at high pressures by CO_2, O_2, and other hydrocarbon molecules. Preliminary measurements suggest ERE-CARS as a potential solution to these limitations.

A schematic diagram of the ERE-CARS system is shown in Fig. 3. Experimental NO ERE-CARS signals generated with this system are compared with calculated NO LIF signals in Fig. 4. The spectral sum of the square root of the ERE-CARS signals and the NO LIF signals are plotted in Fig. 4 for different concentrations of O_2 and CO_2 in a jet flow. It is evident that the NO ERE-CARS signal is essentially independent of the electronic quenching rate whereas the NO LIF signal decreases by more than three orders of magnitudes as the quenching rate increases by a factor of 400-800. The pressure scaling of the NO ERE-CARS and NO LIF signals are shown in Fig. 5, while an ERE-CARS spectrum acquired in a sooty acetylene-air flame is shown in Fig. 6. These measurements show significant promise for the application of ERE-CARS in gas-turbine combustors of interest.

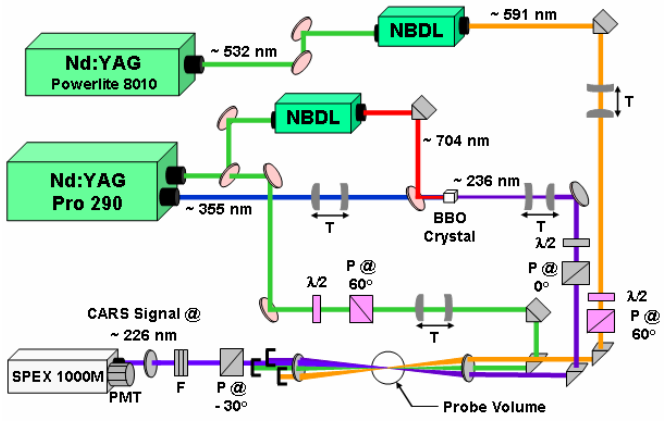

Fig. 3. Schematic diagram of NO ERE-CARS system.

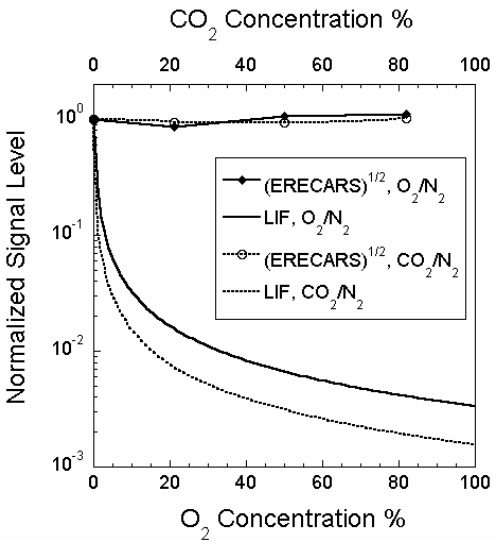

Fig. 4. Dependence of experimental ERE-CARS signals and calculated LIF signals on composition of the $NO/N_2/O_2$ or $NO/N_2/CO_2$ jet flow.

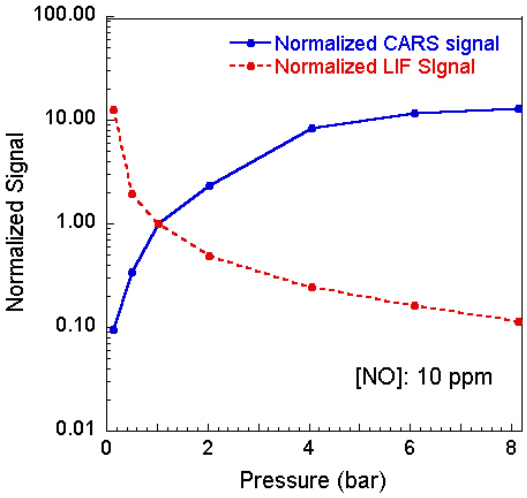

Fig. 5. Pressure-scaling behavior of experimental NO ERE-CARS and calculated NO LIF signals in a high-pressure cell.

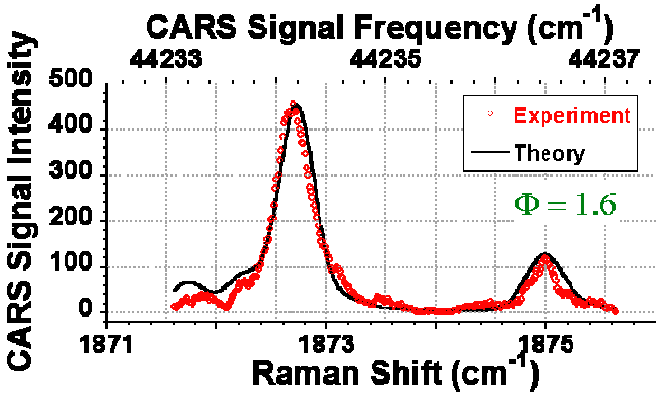

Fig. 6. NO ERE-CARS spectra recorded at a height of 55mm above the burner surface in an C_2H_2/air sooting flame of $\phi = 1.6$ stabilized over the Hencken burner.

SELECTED RECENT PUBLICATIONS

"Application of a Difference-Frequency-Mixing Based Diode-Laser Sensor for Carbon Monoxide Detection in the 4.4-4.8 μm Spectral Region," R.B. Jimenez, J.A. Caton, T.N. Anderson, R.P. Lucht, T. Walther, S. Roy, M.S. Brown, and J.R. Gord, in press, Applied Physics B, 2006.

"Velocity Imaging for the Liquid-Gas Interface in the Near Field of an Atomizing Spray: Proof Of Concept," D.L. Sedarsky, M.E. Paciaroni, M.A. Linne, J.R. Gord, and T.R. Meyer, Opt. Lett. **31**, 906-908, 2006.

"Ballistic Imaging of the Liquid Core for a Steady Jet in Crossflow," M.A. Linne, M. Paciaroni, J.R. Gord, and T.R. Meyer, Appl. Opt. **44**, 6627-6634, 2005.

"Diode-Laser-Based Ultraviolet-Absorption Sensor for High-Speed Detection of the Hydroxyl Radical," T.N. Anderson, R.P. Lucht, T.R. Meyer, S. Roy, and J.R. Gord, Opt. Lett. **30**, 1321-1323, 2005.

"Time-Resolved Dynamics of Resonant and Nonresonant Broadband Picosecond Coherent Anti-Stokes Raman Scattering Signals," S. Roy, T.R. Meyer, and J.R. Gord, Appl. Phys. Lett. **87**, 264103, 2005.

"Measurements of OH Mole Fraction and Temperature up to 20 kHz Using a Diode-Laser-Based UV Absorption Sensor," T.N. Anderson, T.R. Meyer, S. Roy, R.P. Lucht, and J.R. Gord, Appl. Opt. **44**, 6729, 2005.

"10 kHz Detection of CO_2 at 4.5 μm Using Tunable Diode-Laser-Based Difference-Frequency Generation," T.R. Meyer, S. Roy, T.N. Anderson, R.P. Lucht, and J.R. Gord, Opt. Lett. **30**, 3087, 2005.

"Broadband Coherent Anti-Stokes Raman Scattering Spectroscopy of Nitrogen Using a Picosecond Modeless Dye Laser," S. Roy, T.R. Meyer, and J.R. Gord, Opt. Lett. **30**, 3222, 2005.

Abstract for FY05 AFOSR/ARO Contractors Meeting on Chemical Propulsion

EXPERIMENTAL AND COMPUTATIONAL CHARACTERIZATION OF COMBUSTION PHENOMENA

AFOSR Task No. 02PR01COR

Principal Investigator: James R. Gord

Air Force Research Laboratory
AFRL/PRTC Bldg 5
1950 Fifth St
Wright-Patterson AFB OH 45433-7251

SUMMARY/OVERVIEW

Propulsions systems represent a substantial fraction of the cost, weight, and complexity of Air Force aircraft, spacecraft, and other weapon-system platforms. The vast majority of these propulsion systems are powered through combustion of fuel; therefore, the detailed study of combustion has emerged as a highly relevant and important field of endeavor. Much of the work performed by today's combustion scientists and engineers is devoted to the tasks of improving propulsion-system performance while simultaneously reducing pollutant emissions. Increasing the affordability, maintainability, and reliability of these critical propulsion systems is a major driver of activity as well. This research effort is designed to forward the scientific investigation of combustion phenomena through an integrated program of fundamental combustion studies, both experimental and computational, supported by parallel efforts to develop, demonstrate, and apply advanced techniques in laser-based/optical diagnostics and modeling and simulation.

TECHNICAL DISCUSSION

Development of Laser Sources for High-Speed UV and MIR Absorption Spectroscopy Using Sum- and Difference-Frequency Generation. Global instabilities in gas-turbine combustors and augmentors can be as high as 2 kHz, requiring sensors to operate with a bandwidth of at least 4 kHz to satisfy the Nyquist criterion. In addition, ignition/blowout phenomena can occur on much shorter timescales and, based on previous high-speed imaging data, require detection rates of 10-20 kHz. In the current work, compact, high-speed-tunable, diode-laser-based ultraviolet (UV) and mid-infrared (MIR) laser sources for detection of OH, CO, CO_2, and H_2O at rates up to 20 kHz have been developed to study highly unsteady phenomena. The laser source for OH detection is based on sum-frequency generation (SFG) of UV radiation at 313.5 nm by mixing the output of a 763-nm distributed-feedback (DFB) diode laser with a 532-nm high-power, diode-pumped, frequency-doubled Nd:YVO_4 laser in a beta-barium-borate (β-BBO) crystal. The output of this laser source was tuned at 20 kHz across the $P_2(10)$ transition in the $A^2\Sigma^+$-$X^2\Pi$ (v'=0, v''=0) electronic system of OH to demonstrate its potential use for high-speed absorption spectroscopy. The MIR laser source is based on difference-frequency mixing of the 860-nm output of a DFB diode laser with either a 1047-nm Nd:YLF or a 1064-nm Nd:YAG laser in a periodically poled lithium niobate (PPLN) crystal to achieve MIR radiation that can be scanned across CO, CO_2, and H_2O lines at 10 kHz in the wavelength range 4.5-4.8 microns. After initial validation in a laminar Hencken-burner diffusion flame, further demonstrations were performed in the flame zone and exhaust of a JP-8-fueled CFM56 model combustor, as shown in Figs. 1

and 2. Comparison with existing CARS and FTIR data indicates accuracies of 5% at 10 to 20 kHz and demonstrates the potential of SFG- and DFG-based sensors in the UV and MIR for making accurate, time-resolved measurements of multiple species concentrations and temperature for tracking high-speed global instabilities or flame transients.

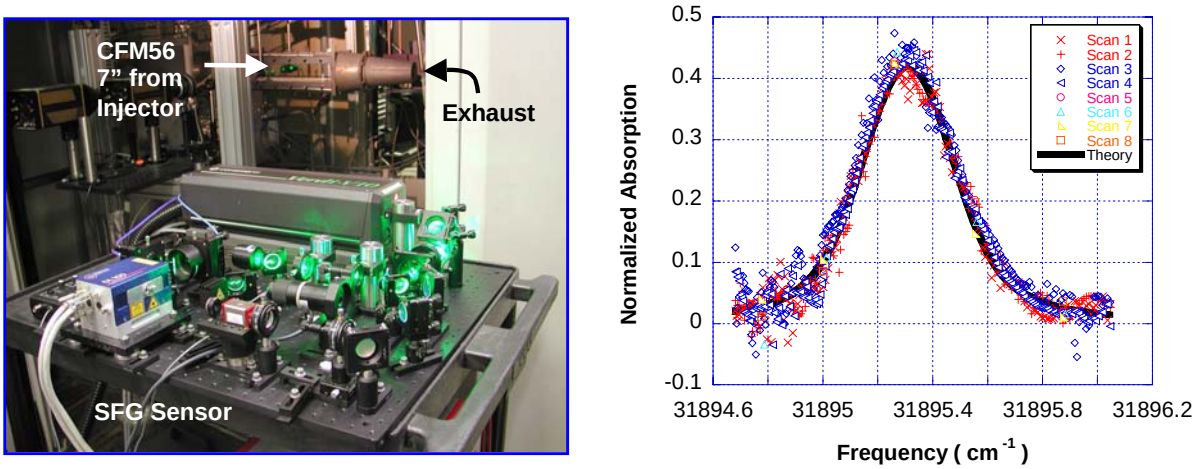

(a) (b)

Figure 1. (a) High-speed OH sensor in CFM56 facility and (b) theoretical fit to multiple OH spectral scans at 20 kHz in CFM56 flame zone.

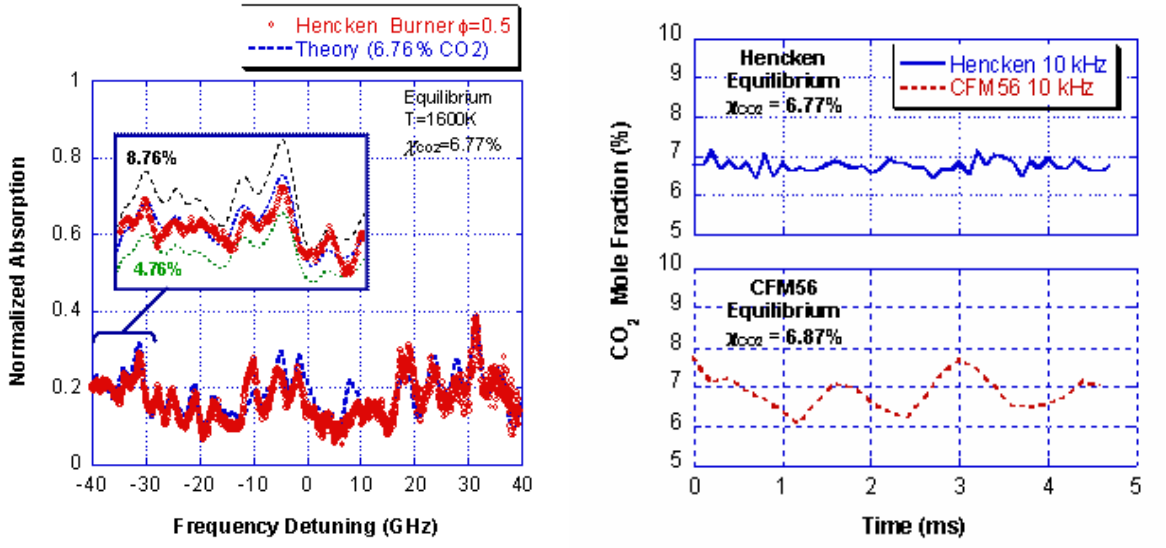

(a) (b)

Figure 2. (a) Validation of CO_2 theoretical model in Hencken burner and (b) 10-kHz CO_2 time series in exhaust of CFM56 combustor.

Ballistic Imaging for Dense-Spray Diagnostics in Gas-Turbine-Engine Applications. Successful modeling and prediction of fuel/air mixture preparation is key to flame stabilization and fuel-conversion efficiency in a wide variety of systems. Recent efforts to benchmark various liquid-spray configurations using double-pulse holography and shadowgraphy have provided some valuable insight but have been limited by the difficulty of extracting information from the dense-spray region. Alternative techniques such as x-ray imaging provide path-averaged information only and require large synchrotron sources available at just a handful of national facilities. Optical imaging of jet breakup focusing on the dense region of liquid fuel sprays would enable significant progress in a critical technology area for military and civilian aircraft propulsion and power generation. In the current work, a femtosecond-laser ballistic-imaging technique was employed in the near field of liquid jets in gaseous crossflows and shown to be

capable of extracting detailed droplet statistics such as Sauter mean diameter. The technique utilizes a 40-fs laser source and a 2-ps Kerr-activated time gate to image ballistic photons transmitted through a dense spray and discriminate against scattered photons. Two innovations in the current work include (1) a two-color approach that takes advantage of the large bandwidth available in the 40-fs pulse and (2) a double-pulse approach that will allow measurement of droplet velocities in the dense-spray region. Measurements were performed under a variety of liquid-jet diameters, gaseous-crossflow velocities, and liquid-air momentum ratios. A sample image with 40-μm resolution is shown in Fig. 3, along with droplet statistics for various crossflow velocities. An ongoing project will employ the technique to collect benchmark data in a test cell at realistic gas-turbine conditions for spray modeling and validation.

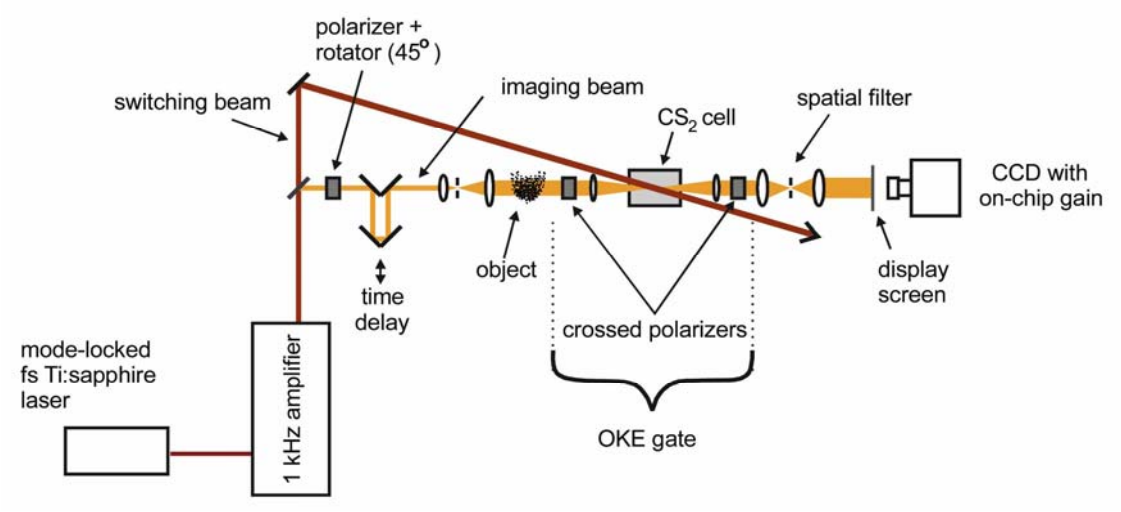

(a)

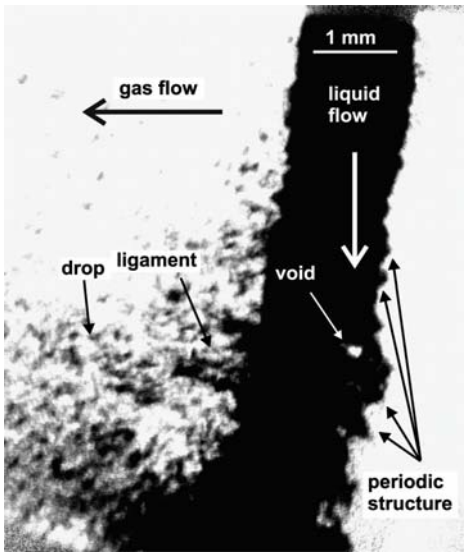

(b)

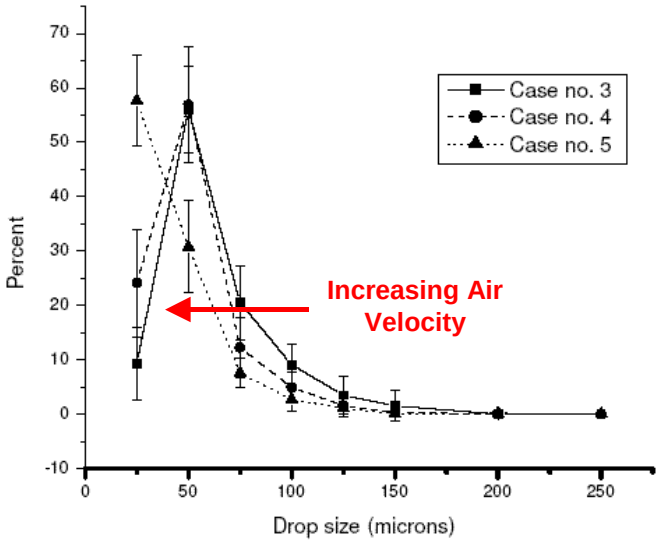

(c)

Figure 3. (a) Schematic diagram of ballistic-imaging set-up, (b) sample jet-in-crossflow image, and (c) droplet statistics as a function of increasing air velocity.

Broadband Picosecond Coherent Anti-Stokes Raman Scattering Spectroscopy of Nitrogen Using a Modeless Dye Laser. There are three potential advantages of short-pulse coherent anti-Stokes Raman scattering (CARS) spectroscopy: (1) it improves accuracy by reducing or eliminating the nonresonant contribution to the CARS signal when the probe beam is delayed with respect to the pump beam, (2) it minimizes the effects of collisions on the CARS signal,

thereby reducing modeling uncertainty and increasing signal-to-noise ratio, and (3) it improves sensitivity and may enable the detection of minor species through reduction or elimination of interference from the nonresonant background. These advantages could significantly enhance the performance of CARS thermometry in high-pressure, liquid-fueled combustors of practical interest by overcoming known limitations of nanosecond-based systems. In the current work, broadband picosecond CARS spectroscopy of nitrogen is demonstrated using a 135-ps pump beam and a 115-ps Stokes beam. The broadband picosecond Stokes beam at ~607 nm with a full width half maximum (FWHM) of 5 nm (136 cm^{-1}) is generated by pumping a modeless dye laser with a nearly transform-limited, 532-nm pump beam from a Nd:YAG regenerative amplifier. To our knowledge this is the first experimental demonstration of broadband picosecond CARS spectroscopy. This approach enables single-shot thermometry in unsteady flows, in contrast with scanning CARS using picosecond optical-parametric-amplifier-based, distributed-feedback, or synchronously pumped dye-laser systems. A schematic diagram of the system and room-temperature nitrogen data are depicted in Fig. 4.

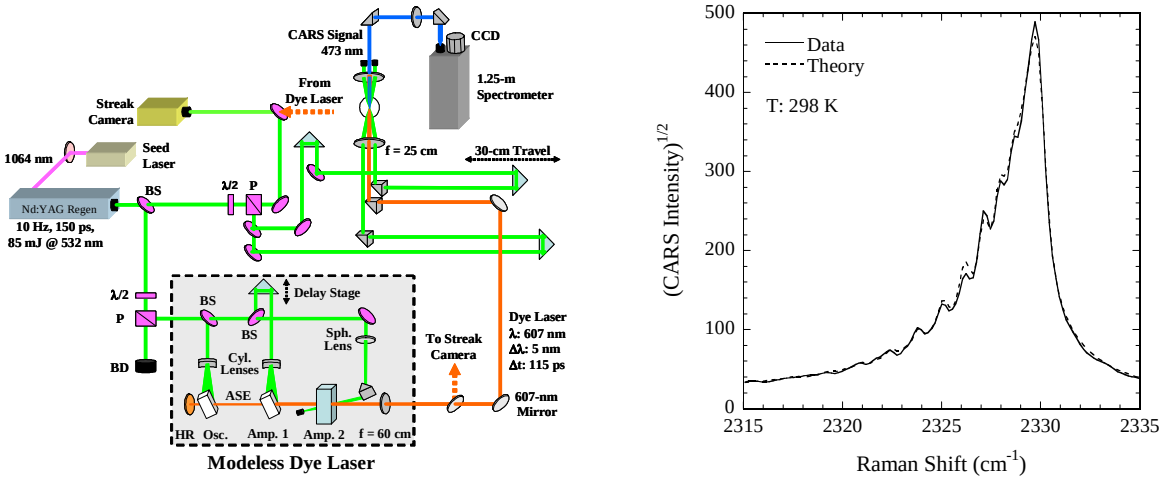

Figure 4. (a) Schematic diagram of broadband picosecond CARS system and (b) experimental and theoretical broadband coherent anti-Stokes Raman scattering spectrum of nitrogen at room temperature.

SELECTED RECENT PUBLICATIONS

"Broadband Coherent Anti-Stokes Raman Scattering Spectroscopy of Nitrogen Using a Picosecond Modeless Dye Laser," S. Roy, T.R. Meyer, and J.R. Gord, submitted for publication in Optics Letters, 2005.

"10-kHz Detection of CO_2 at 4.5 μm Using Diode-Laser-Based Difference-Frequency Generation," T.R. Meyer, S. Roy, T.N. Anderson, R. Barron-Jimenez, R.P. Lucht, and J.R. Gord, submitted for publication in Optics Letters, 2005.

"Real-Time Measurements of OH Concentration and Temperature in a C_2H_4-Air Flame Using a Diode-Laser-Based Ultraviolet Absorption Sensor," T.A. Anderson, T.R. Meyer, S. Roy, R.P. Lucht, and J.R. Gord, submitted for publication in Applied Optics, 2005.

"Ballistic Imaging of the Liquid Core for a Steady Jet in Crossflow," M.A. Linne, M. Paciaroni, J.R. Gord, T.R. Meyer, submitted for publication in Applied Optics, 2005.

"Dual-Pump Dual-Broadband CARS for Exhaust-Gas Temperature and $CO_2/O_2/N_2$ Concentration Measurements in Model Gas-Turbine Combustors," T.R. Meyer, S. Roy, R.P. Lucht, and J.R. Gord, accepted for publication in Combustion and Flame, 2005.

"Diode-Laser-Based Ultraviolet-Absorption Sensor for High-Speed Detection of the Hydroxyl Radical," T.A. Anderson, R.P. Lucht, T.R. Meyer, S. Roy, and J.R. Gord, Opt. Lett. **30**, 1321 (2005).

"Simultaneous Planar Laser-Induced Incandescence, OH Planar Laser-Induced Fluorescence, and Droplet Mie Scattering in Swirl-Stabilized Spray Flames," T.R. Meyer, S. Roy, V.M. Belovich, E. Corporan, and J.R. Gord, Appl. Opt. **44**, 445 (2005).

"Dual-Pump Dual-Broadband Coherent Anti-Stokes Raman Scattering in Reacting Flows," S. Roy, T. R. Meyer, R.P. Lucht, M. Afzelius, P.-E. Bengtsson, and J.R. Gord, Opt. Lett. **29**, 1843 (2004).

Abstract for FY04 AFOSR/ARO Contractors Meeting on Chemical Propulsion

EXPERIMENTAL AND COMPUTATIONAL CHARACTERIZATION OF COMBUSTION PHENOMENA

AFOSR Task No. 02PR01COR

Principal Investigator: James R. Gord

Air Force Research Laboratory
AFRL/PRTC Bldg 5
1950 Fifth St
Wright-Patterson AFB OH 45433-7251

SUMMARY/OVERVIEW

Propulsions systems represent a substantial fraction of the cost, weight, and complexity of Air Force aircraft, spacecraft, and other weapon-system platforms. The vast majority of these propulsion systems are powered through combustion of fuel; therefore, the detailed study of combustion has emerged as a highly relevant and important field of endeavor. Much of the work performed by today's combustion scientists and engineers is devoted to the tasks of improving propulsion-system performance while simultaneously reducing pollutant emissions. Increasing the affordability, maintainability, and reliability of these critical propulsion systems is a major driver of activity as well. This research effort is designed to forward the scientific investigation of combustion phenomena through an integrated program of fundamental combustion studies, both experimental and computational, supported by parallel efforts to develop, demonstrate, and apply advanced techniques in laser-based/optical diagnostics and modeling and simulation.

TECHNICAL DISCUSSION

While this AFOSR-funded program involves numerous ongoing investigations, just a few recent advances are described in this abstract. Many other ongoing activities have been reviewed during recent AFOSR/ARO Contractors Meetings and are not discussed at length here.

Simultaneous OH PLIF and LII for Visualization of Flame Structure and Soot Inception in Swirl-Stabilized Liquid-Spray Flames. Much of the fundamental knowledge concerning soot formation is derived from investigations of laminar diffusion flames, with only a limited number of studies focusing on unsteady effects. The importance of considering unsteadiness and fluid-flame interactions was demonstrated by Shaddix et al. [Combust. Flame 99:723-732] who found that a forced methane/air diffusion flame produced a four-fold increase in soot volume fraction as compared with a steady flame having the same mean fuel-flow velocity. The goal of the current work is to study soot formation in the highly dynamic environment of a swirl-stabilized JP-8-fueled model combustor, which is characterized by high shear stresses and turbulent intensities that result in vortex breakdown and large-scale unsteady motions. This goal is accomplished by simultaneous imaging of the soot volume fraction and hydroxyl-radical (OH) distribution using laser-induced incandescence (LII) and OH planar laser-induced fluorescence (PLIF), respectively. Mie scattering from large droplets, which appears in the OH images but does not preclude signal interpretation, is used to a limited extent as a spray diagnostic. As shown in Fig. 1, the experimental set-up includes an Nd:YAG for saturated LII at 532 nm and a narrowband dye laser for OH PLIF using the $Q_1(9)$ line in the 1-0 band of the A-X system.

The injector geometry and sample instantaneous OH-PLIF images for JP-8 and a non-aromatic liquid fuel are shown in Fig. 2 at an equivalence ratio (ϕ) of 0.8. Such images provide a clear indication of the intermittency within the primary flame zone and are useful for characterizing the statistical behavior in terms of probability density functions. It is found, for example, that large-scale structures play a key role in the soot formation process. Intermittent regions of rich premixed fuel and air develop between the primary flame layer and recirculation zone that serve as sites for soot inception. The rate of soot production is dependent upon the frequency and spatial extent of these regions, while the rate of soot oxidation is dependent upon the availability of oxygen and OH in primary zone and recirculation region. Hence, the overall soot volume fraction is highly sensitive to the dynamics of the injection process as well as to the local, unsteady equivalence ratio. The importance of the former is highlighted by differences in the vaporization and soot formation characteristics of JP-8 versus non-aromatic fuels, as shown in Figs. 2(b) and 2(c).

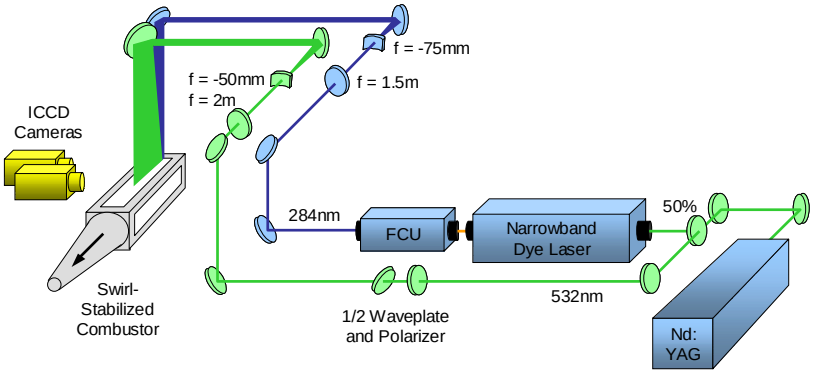

Fig. 1. Simultaneous OH PLIF and LII in atmospheric-pressure, swirl-stabilized, JP8-fueled, model gas-turbine combustor.

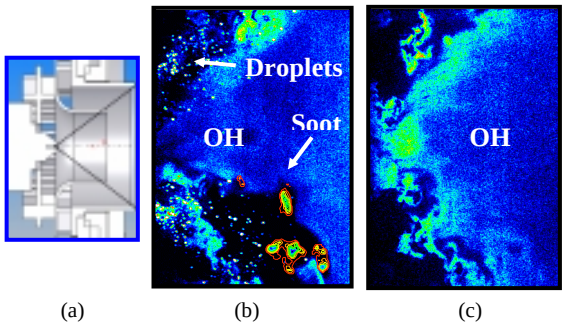

Fig. 2. (a) Dual-radial swirl cup with center-mounted pressure-swirl injector, (b) primary zone with JP-8 at ϕ = 0.8, and (c) primary zone with non-aromatic fuel at ϕ = 0.8.

In studies of soot-mitigating additives, performed in collaboration with the Fuels Branch of ARFL, the simultaneous OH-PLIF and LII measurements were used to determine whether changes in soot production result from changes in the chemical or physical properties of the fuel. Figs. 3(a) and 3(b) demonstrate the ability of the current measurement system to track local equivalence ratio and soot production, respectively. Using a droplet-free region in the recirculation zone, the time- and spatially averaged OH-PLIF signal is plotted with respect to equivalence ratio and compared with an equilibrium calculation. This provides a calibration for JP-8 that can be used qualitatively to track changes in equivalence ratio. The data in Fig. 3(a) include corrections for the effects of collisional

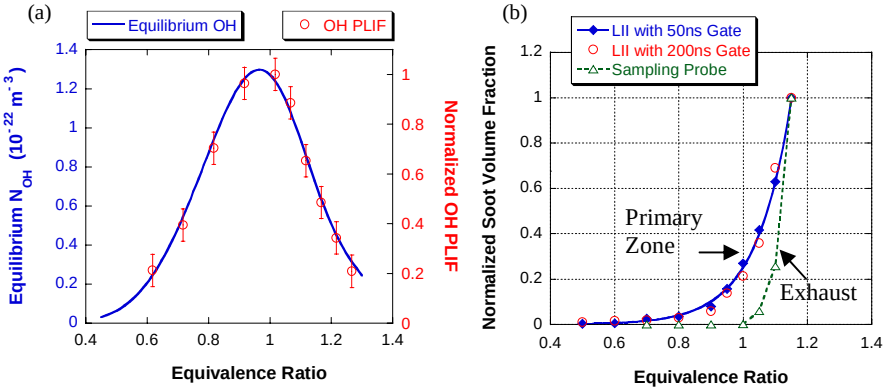

Fig. 3. (a) Fit of OH data in recirculation region with equilibrium calculations and (b) comparison of normalized soot volume fraction in primary zone with particle counts in the exhaust stream.

quenching and Boltzmann-fraction variations on the OH-PLIF signal. The LII data in Fig. 3(b) show an exponential increase of the soot volume fraction in the primary zone with respect to equivalence ratio. A subsequent test using an increased LII-gate period demonstrates minimal particle-size bias and measurement repeatability. Note that the exhaust-gas sampling probe displays a threshold effect at about ϕ = 1.0, below which soot in the exhaust is effectively oxidized by OH and O_2 due to long residence times.

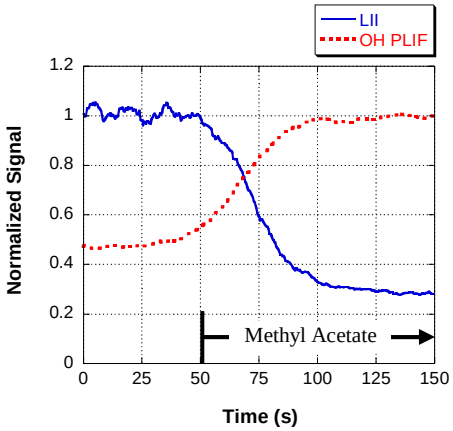

Fig. 4. Drop in soot due to methyl acetate addition corresponds to decrease in ϕ as verified by OH PLIF.

Since the dependence of soot on equivalence ratio is exponential, slight changes in equivalence ratio could easily be mistaken for changes in soot particle counts in the exhaust stream. This highlights the importance of tracking equivalence ratio while performing studies of soot-mitigating additives. An example is shown in Fig. 4 where methyl acetate is added to the fuel during a test. Note the large decrease in soot volume fraction during methyl-acetate addition, as measured by LII; this corresponds to a large decrease in particle counts from the sampling probe. Note also the increase in OH-PLIF signal that, according to the results of Fig. 3(a), indicates that the fuel mixture is becoming leaner. A certain ambiguity exists, however, because the final equivalence ratio could lie on either side of the peak OH signal. Using the exponential fit to the data in Fig. 3(b), however, the change in LII signal corresponds to an equivalence ratio that is slightly on the rich side of the OH peak. An overall equivalence-ratio decrease of 0.123 due to methyl-acetate addition is measured to within 1% for both the OH-PLIF and LII data, and to within 10% of flow calculations. The agreement between OH-PLIF and LII data indicates that methyl acetate in the current study did not have an effect on soot production, except for its effect on equivalence ratio. One can envision, therefore, the use of a combined LIF and LII system to track the performance of soot-mitigating additives without uncertainties in equivalence ratio.

Detection of Atomic Hydrogen in Reacting Flows Using Two-Color, Two-Photon Picosecond Laser-Induced Polarization Spectroscopy. Atomic hydrogen is an important species in hydrocarbon-based chemically reacting flows because of its high reactivity and diffusivity. In non-premixed flames interacting with vortices, the time evolution of the hydrogen atom closely follows that of heat release during the interaction and, therefore, will reveal information concerning the heat-release rate during the interaction process. Moreover, the hydrogen atom may play an important role in the formation of soot in hydrocarbon combustion. For example, in low-pressure diamond-synthesis environments, the hydrogen atom plays a significant role in determining the growth rate and quality of the diamond film. Therefore, the measurement of atomic-hydrogen concentration in flames is of fundamental importance in understanding relevant chemical and mass-transfer processes. In the current work, two-color, two-photon laser-induced polarization spectroscopy (LIPS) of atomic hydrogen using nearly transform-limited picosecond laser pulses is demonstrated. The use of short laser pulses (laser pulse width τ_L < characteristic collision time τ_C) significantly decreases the collision-rate dependence of the LIPS signal as compared to long laser pulses ($\tau_L > \tau_C$) interacting with atoms or molecules. The broadening of the spectral lines and the shift in transition frequencies with laser power is also investigated. This is, to our knowledge, the first reported two-color, two-photon LIPS experiment using

picosecond lasers for the detection of atomic hydrogen in reacting flows. The LIPS spectra of atomic hydrogen for pump beam energies of ~13 μJ and ~30 μJ are shown in Figure 6. The spectral line shapes shown in Fig. 5 were normalized to have maximum values of unity. Spectral broadening of the resonance line shape with laser power and the slight shift in transition frequency due to the ac Stark shift are evident in Fig. 5.

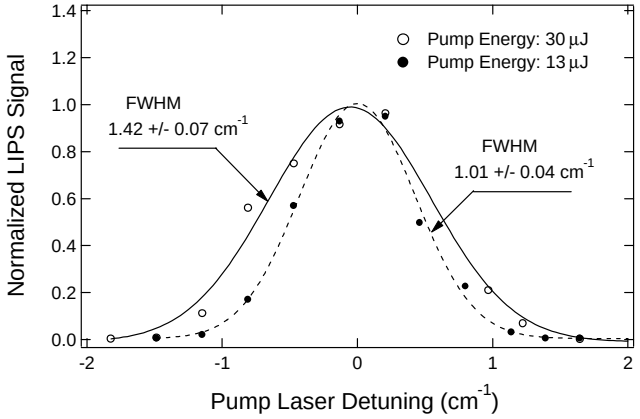

Fig. 5. LIPS spectrum of atomic hydrogen at two laser powers in a near-adiabatic hydrogen-air flame stabilized on a Hencken burner. The LIPS signal is normalized to have a maximum value of unity. The lines show Gaussian profiles fit through the experimental data points.

SELECTED RECENT PUBLICATIONS

"Dual-Pump Dual-Broadband Coherent Anti-Stokes Raman Spectroscopy," S. Roy, T. R. Meyer, R. P. Lucht, M. Afzelius, P.-E. Bengtsson, and J. R. Gord, accepted for publication in Optics Letters, 2004.

"Simultaneous PLIF/PIV Investigation of Vortex-Induced Annular Extinction in H_2-Air Counterflow Diffusion Flames," T.R. Meyer, G.J. Fiechtner, S.P. Gogineni, C.D. Carter, and J.R. Gord, Exp. Fluids **36**, 259 (2004).

"PIV/PLIF Investigation of Two-Phase Vortex-Flame Interactions: Effects of Vortex Size and Strength," A. Lemaire, T.R. Meyer, K. Zähringer, J.R. Gord, and J.C. Rolon, Exp. Fluids **36**, 36 (2004).

"Triple-Pump Coherent Anti-Stokes Raman Scattering (CARS): Temperature and Multiple-Species Concentration Measurements in Reacting Flows," S. Roy, T. R. Meyer, M. S. Brown, V. N. Velur, R. P. Lucht, and J. R. Gord, Opt. Comm. **224**, 131 (2003).

"Analysis of Transient-Grating Signals for Reacting-Flow Applications," M. S. Brown, Y. Li, W. Roberts, and J. R. Gord, Appl. Opt. **42**, 566 (2003).

"Lifetime Measurement and Calibration from Pressure-Sensitive Paint Luminescence Images," T. F. Drouillard II, M. A. Linne, L. P. Goss, J. R. Gord, and G. J. Fiechtner, Rev. Sci. Instrum. **74**, 276 (2003).

"Insights into Non-Adiabatic Flame Temperatures During Small-Scale-Vortex/Flame Interactions," V. R. Katta, T. R. Meyer, J. R. Gord, and W. M. Roquemore, Combust. Flame **132**, 639 (2003).

"Vortex-Induced Flame Extinction in Two-Phase Counterflow Diffusion Flames Using CH PLIF and PIV," A. Lemaire, T. R. Meyer, K. Zähringer, J. C. Rolon, and J. R. Gord, Appl. Opt. **42**, 2063 (2003).

"Dual-Pump Coherent Anti-Stokes Raman Scattering Temperature and CO_2 Concentration Measurements," R. P. Lucht, V. N. Velur, C. D. Carter, K. D. Grinstead, J. R. Gord, P. M. Danehy, G. J. Fiechtner and R. L. Farrow, AIAA J. **41**, 679 (2003).

Abstract for FY03 AFOSR/ARO Contractors Meeting on Chemical Propulsion

EXPERIMENTAL AND COMPUTATIONAL CHARACTERIZATION OF COMBUSTION PHENOMENA

AFOSR Task No. 02PR01COR

Principal Investigator: James R. Gord

Air Force Research Laboratory
AFRL/PRTS Bldg 490
1790 Loop Rd N
Wright-Patterson AFB OH 45433-7103

SUMMARY/OVERVIEW

Propulsions systems represent a substantial fraction of the cost, weight, and complexity of Air Force aircraft, spacecraft, and other weapon-system platforms. The vast majority of these propulsion systems are powered through combustion of fuel; therefore, the detailed study of combustion has emerged as a highly relevant and important field of endeavor. Much of the work performed by today's combustion scientists and engineers is devoted to the tasks of improving propulsion-system performance while simultaneously reducing pollutant emissions. Increasing the affordability, maintainability, and reliability of these critical propulsion systems is a major driver of activity as well. This research effort is designed to forward the scientific investigation of combustion phenomena through an integrated program of fundamental combustion studies, both experimental and computational, supported by parallel efforts to develop, demonstrate, and apply advanced techniques in laser-based/optical diagnostics and modeling and simulation.

TECHNICAL DISCUSSION

While this AFOSR-funded program involves numerous ongoing investigations, just a few recent advances are described in this abstract. Many other ongoing activities have been reviewed during recent AFOSR/ARO Contractors Meetings and are not discussed at length here.

Continuing Collaborative Studies of Vortex-Flame Interactions with École Centrale Paris and ONERA. The investigation of vortex-perturbed counterflow diffusion flames is critical to our understanding of fundamental combustion processes. These interactions represent idealized turbulent combustion phenomena, and their studies will drive the development and evaluation of simplified models to be used in design codes for practical combustion systems. Here we discuss continuing work in two configurations: a counterflow flame perturbed by multiple colliding vortices and a two-phase counterflow flame perturbed by a single vortex.

Initial work in the multiple-colliding-vortex configuration has been focused on the generation of small-scale multiple-vortex-flame interactions to simulate turbulent conditions with improved fidelity. Because the counter-propagating-vortex configuration induces a stationary vortex-flame interaction, the early stages of interaction represent an idealized vortex-induced flame extinction. Current work in this area has been designed to explore the feasibility of extracting a single universal criterion for local flame extinction induced by dynamic strain.

Changes in the structure of a flat counterflow diffusion flame during its interaction with multiple incoming vortices have been investigated using planar laser-induced fluorescence (PLIF) of the hydroxyl radical (OH) and an in-house time-dependent computational fluid

dynamics code with chemistry (CFDC) known as UNICORN. Excellent agreement between experimental and computational data has been achieved, as documented in Figure 1. Three variables were investigated for various incoming vortex velocities to characterize the observed quenching process: the air-side strain rate, fuel-side strain rate, and the scalar dissipation rate. Here, strain rates are defined as the component of the velocity gradient normal to the flame surface, and scalar dissipation is the vector product of the fuel concentration gradient with itself. It is found that none of these variables can individually characterize the quenching process associated with unsteady flames. It is proposed instead that a variable proportional to the air-side strain rate and inversely proportional to the temperature-drop rate at extinction could characterize the unsteady quenching process. Figure 2 shows that the air-side strain rate increases linearly with the temperature-drop rate. Since temperature drop directly correlates the balance between the reactant influx and its consumption in the flame zone (extent of non-equilibrium nature of the reactions), Fig. 2 suggests that the quenching value of the air-side strain rate increases with the extent of non-equilibrium chemistry taking place in the flame zone. By defining a variable that is proportional to the air-side strain rate and inversely proportional to the temperature-drop rate, a universal term for describing the quenching process in unsteady flames can be obtained. For example:

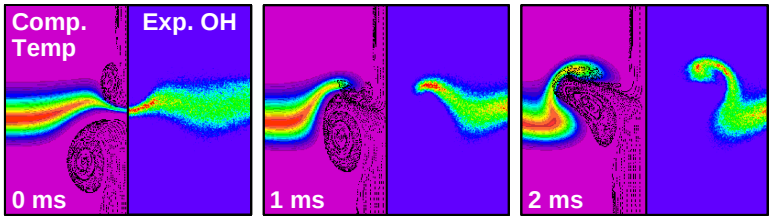

Figure 1. Computed temperature vs. OH PLIF data for a flat counterflow diffusion flame perturbed by multiple vortices.

$$\sigma = T_\infty \frac{K_a}{\left(dT/dt\right)_{ext}}$$

where σ is the extinction parameter, K_a is the air-side strain rate, T is temperature, t is time, and T_∞ is the unperturbed temperature.

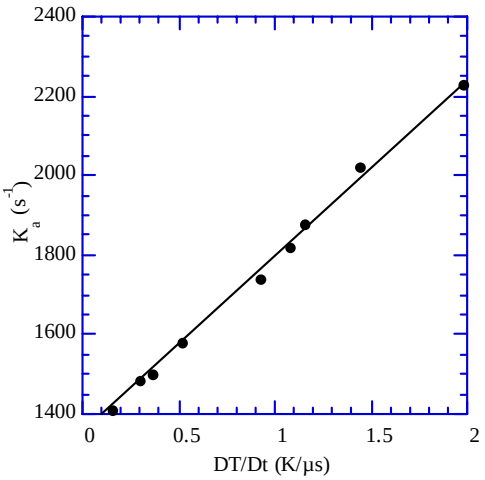

Figure 2. Proportionality of air-side strain rate with temperature-drop rate at extinction.

In the two-phase vortex flame configuration (Fig. 3), early work was focused on demonstrating the experimental technique and discerning the effects of fuel composition, droplet seeding levels, and PAH fluorescence on the CH PLIF signal. Recent work has been focused on detailed analyses of the *rate* of CH layer extinction and the evolution of flame surface area during the two-phase counterflow flame inter-

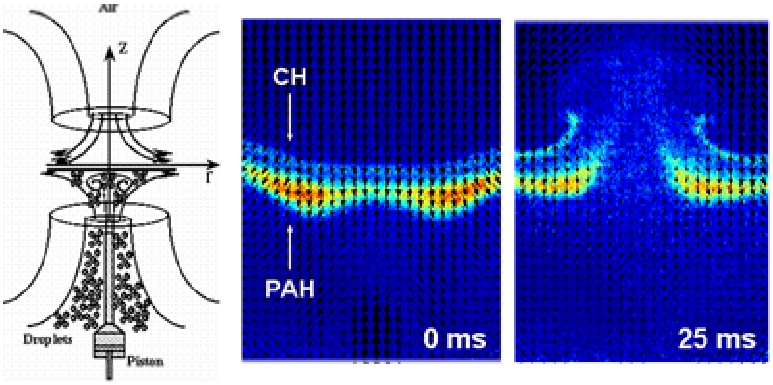

Figure 3. Flow configuration (left) and simultaneous PLIF/PIV images during two-phase vortex-flame interactions (middle and right).

action with fuel-side vortices of varying size and strength. Detailed analysis of the strain rate along the centerline has also been performed using PIV data acquired simultaneously with CH PLIF, as shown on the left in Fig. 4. Vortices of similar initial circulation but differing size show widely disparate peak strain rates and CH decay rates due to varying levels of flame-induced vortex dissipation. As shown in the center plot of Fig. 4, the CH decay rate is nearly linear in time with increasing slopes at higher fuel-side strain rates. These data are useful for evaluating the extinction behavior of two-phase vortex-flame interactions in the context of the universal criterion suggested above as modified for the case of a single fuel-side vortex.

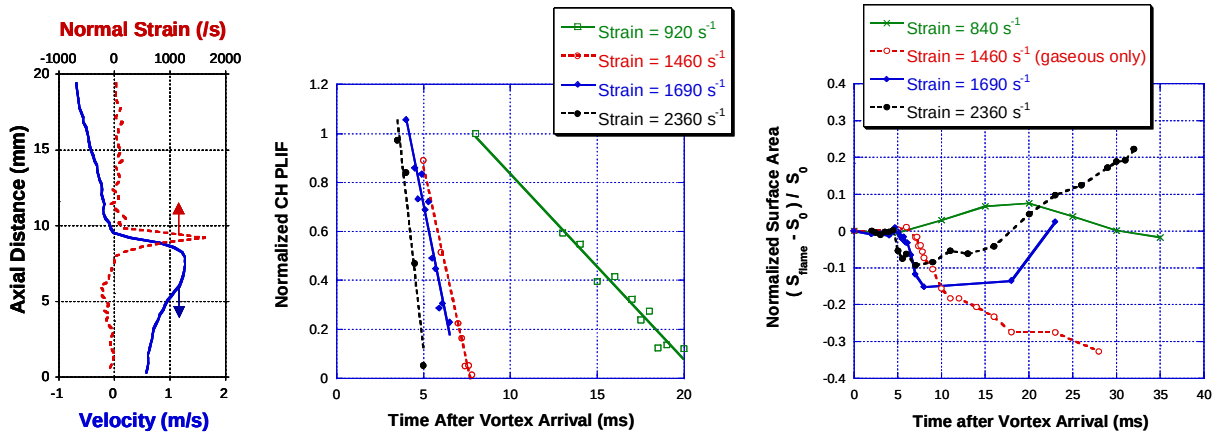

Figure 4. Experimentally measured normal strain rate along the centerline (left), normalized CH PLIF as a function of strain rate and time after vortex arrival (middle), and evolution of normalized flame surface area as a function of strain rate and time after vortex arrival (right).

Dual-Pump, Dual-Broadband Coherent Anti-Stokes Raman Scattering for Characterization of Liquid-Fueled Combustors. Our FY02 abstract described collaborative development with Prof. Bob Lucht (Purdue University) and his team at Texas A&M University of triple-pump CARS. That effort has been expanded to yield a dual-pump, dual-broadband CARS system for simultaneous detection of temperature and three species concentrations in reacting flows. In this CARS system, the rotational transitions of N_2/O_2 and the rovibrational transitions of N_2/CO_2 are probed. The CARS spectra of each molecule pair are observed within a distinct wavelength band, allowing two molecule pairs to be measured simultaneously using a detection system that includes two spectrometers and two cameras. Since nitrogen is a common species in each molecule pair, it can be used as a reference for normalizing species concentrations and for

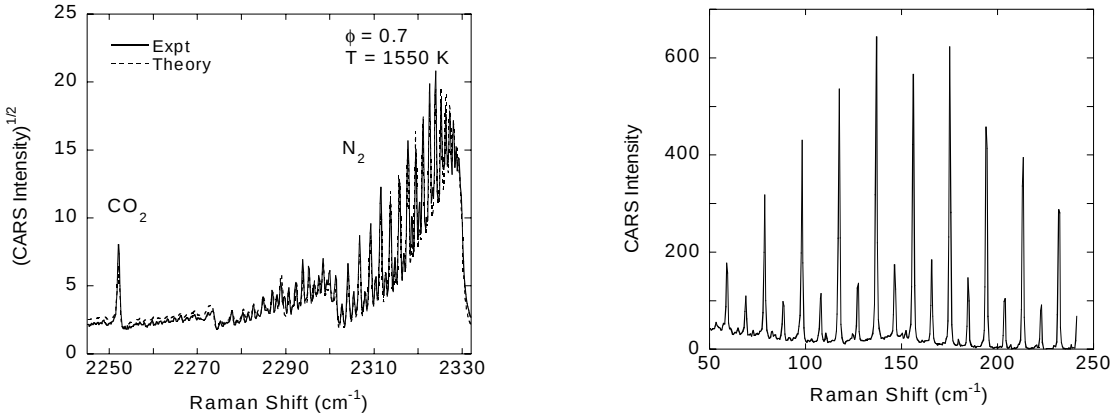

Figure 5. CARS signals obtained in the exhaust stream of the CFM56 combustor. Rovibrational spectra for N_2 and CO_2 are depicted on the left. Rotational spectra for N_2 and O_2 acquired simultaneously with the N_2/CO_2 spectra are depicted on the right.

improving the accuracy and dynamic range of temperature measurements. Demonstration of this measurement technology has been accomplished in the exhaust of a liquid-fueled, swirl-stabilized CFM56 combustor. These measurements were performed to investigate the exhaust-stream temperatures and CO_2 concentrations for various jet fuels over a range of equivalence ratios. The effects of fuel additives on these combustor parameters were explored as well. Representative data are captured in Figure 5.

Transient-Grating Thermometry in a Trapped-Vortex Combustor. Transient grating spectroscopy (TGS, also known as laser-induced thermal acoustics or LITA) is a nonlinear optical technique that can be applied to measure gas temperature, sound speed, thermal diffusivity, and various other parameters of interest in reacting flowfields. Two pulsed pump beams derived from the same laser are crossed to generate a laser-induced grating in the probe volume via nonresonant absorption. The local hydrodynamic response produces two counter-propagating sound waves that scatter a phase-matched probe beam to yield a beam-like signal. In turbulent environments, single-shot signals are acquired and analyzed to produce probability density functions (PDF's) of the inferred temperature.

As part of our continuing effort to develop and apply this technique, transient grating thermometry has been performed in the rich flame zone of a TVC operating under turbulent, pressurized, JP-8-fueled conditions. Measurements were accomplished at pressures of 50, 75, and 100 psi with local equivalence ratios in the range 1–1.25. The pump beams were derived from the 565-nm output of a Nd:YAG-pumped dye laser. The cw output of a vanadate laser (532 nm) provided the probe beam. While the pump lasers were not tuned to a particular molecular resonance, the detected signals showed clear signs of thermalization and the absence of nonresonant electrostriction. Soot particles and soot precursors are the likely absorbers responsible for signal generation. Beam steering was clearly evident in the form of variable pointing and random spatial modulation of the exiting beams. Due to such adverse affects, signal was not obtained on all laser shots; however, useful signals were generated with sufficient frequency to permit meaningful temperature measurements.

A typical single-shot signal is depicted in Figure 6. A temperature PDF constructed from ~800 analyzed single shots is depicted in Figure 7. The resulting PDF is centered at 2000 K. The breadth of the PDF largely reflects the local dynamic nature of the reaction zone as pockets of fluid in different relative states of combustion maturity pass through the probe volume. The far wings of the PDF also contain contributions from electronic noise (particularly at high frequency) and processing noise (particularly at low frequency). Note that all signals were processed with no discrimination against those with very low signal-to-noise ratios.

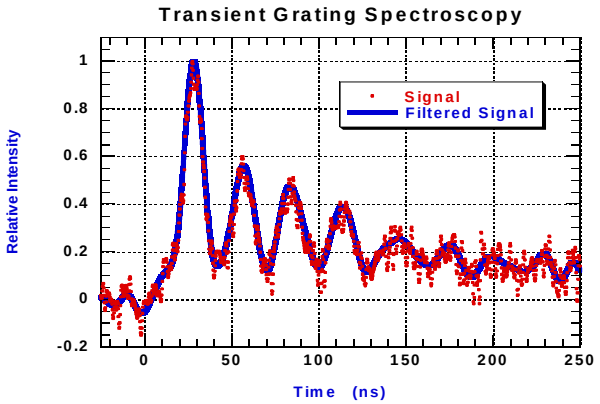

Figure 6. Single-shot TGS signal acquired in the rich flame zone of a TVC operating under turbulent, pressurized, JP-8-fueled conditions.

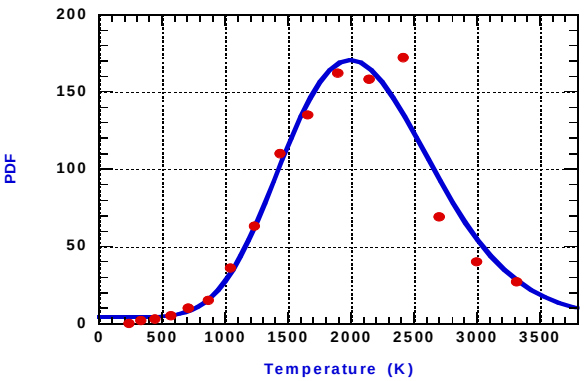

Figure 7. Temperature PDF constructed through analysis of ~800 single-shot signals acquired in a TVC operating at a pressure of 100 psi.

Invited Paper “Emerging Combustion Diagnostics” presented in January 2001 at the 39th American Institute of Aeronautics and Astronautics Aerospace Sciences Meeting and Exhibit in Reno NV

AIAA-2001-0784

EMERGING COMBUSTION DIAGNOSTICS

James R. Gord*
Air Force Research Laboratory
Propulsion Directorate
Wright-Patterson Air Force Base OH

Gregory J. Fiechtner†
Sandia National Laboratories
Combustion Research Facility
Livermore CA

Abstract

While optical diagnostic techniques have been applied with great success to the fundamental study of combustion chemistry and physics in the laboratory, the challenges afforded by real-world propulsion systems demand continuing innovation if such techniques are to be adapted and transitioned for use in engineering test and on-board monitoring and control applications. A desire to achieve measurement tools in new spectral territory that exploit limited available optical access and provide high data-acquisition bandwidth has motivated the development efforts described in this paper. An ultranarrowband, mid-infrared optical parametric oscillator, terahertz transmitters and receivers for studies in the far-infrared, and high-speed imaging systems based on modelocked lasers and high-framing-rate cameras represent just a few of the potential solutions now under development for current and future combustion and propulsion applications.

Introduction

Much of the work performed by today's combustion scientists and engineers, particularly those associated with gas-turbine and internal-combustion-powered propulsion, is devoted to the tasks of improving propulsion-system performance while simultaneously reducing pollutant emissions. Increasing the affordability, maintainability, and reliability of these propulsion systems is also a driver of activity. Advanced measurement techniques that exploit laser-based or other optical approaches have become well-established tools to aid the accomplishment of these tasks.[1]

These non-invasive measurement approaches are often suited for visualizing complex reacting flowfields and quantifying key chemical-species concentrations and fluid-dynamic parameters. The fundamental information these techniques provide is essential for achieving a detailed understanding of the chemistry and physics of combustion processes. Furthermore, these data are critical for validating combustion models and combustor-design codes that promise to usher in a new era in propulsion-system development.

While conditions in the laboratory phase of diagnostics development are often ideal and well controlled, combustor-facility applications involve conditions characteristic of actual engine hardware. Challenges include extreme environmental conditions (heat, vibration, acoustics, etc.), limited optical access, tight geometric constraints, little operational space, fully developed turbulence, two-phase flows, soot formation, high pressure, collisional quenching and energy redistribution, optical thickness, beam steering, high background luminosity, and scattering and spectral interferences. An approach to the design process that addresses these significant challenges is depicted in Fig. 1. The elements in this figure represent the transition from basic-research activities (termed 6.1 in the Air Force and Department of Defense) through exploratory development (termed 6.2) and applied engineering (termed 6.3). At the basic-research level, new diagnostic approaches are developed and tested in conjunction with extensive simulation-and-modeling efforts. Techniques are "cross-validated" through studies of fundamental combustion processes in

*Principal Research Chemist, Member AIAA
†Mechanical Engineer, Associate Fellow AIAA

laboratory rigs that provide favorable optical conditions while remaining computationally tractable. Axisymmetric burners that provide ample optical access and well-defined boundary conditions represent such test articles. The measurement and computational tools designed, tested, and matured through this basic research are applied subsequently to hardware testing and evaluation in the 6.2 phase of the effort. At the 6.3 level, sensor platforms based on these diagnostic approaches are incorporated for on-board propulsion-system monitoring and control.

This approach has been applied by many research organizations in the combustion community to yield an impressive toolbox of powerful diagnostic techniques and some tremendous success stories; however, the inherent complexity of propulsion systems and the combustion processes that drive them demand continuing innovation. Efforts to develop and apply the measurement techniques required for addressing current and future propulsion challenges are the subject of this technical session and this paper. This particular paper is not intended to serve as an exhaustive review of diagnostics-development activity across the broad spectrum of the propulsion and combustion communities. Rather it highlights some continuing development efforts underway at the Air Force Research Laboratory at Wright-Patterson Air Force Base.

The paper continues with a brief description of efforts to develop and apply an ultranarrowband optical parametric oscillator for combustion measurements in the mid-infrared region. This program has been accomplished in cross-directorate cooperation between the Air Force Research Laboratory's Propulsion and Sensors Directorates. Researchers with Aculight Corporation have spearheaded the effort. The section that follows briefly documents a program involving Propulsion-Directorate scientists with teams at Picometrix, Inc., and Innovative Scientific Solutions, Inc., to provide transmitters and receivers for applying coherent terahertz radiation to study combustion processes and condensed-phase fuels in the far-infrared spectral region. Developments in high-speed digital imaging achieved through the marriage of ultrafast, high-repetition-rate lasers with novel camera architectures is more fully described in the final section of the paper.

At least three themes have motivated the development efforts described in this paper. These themes are a natural response to the challenges associated with advancing the art and the science of combustion and propulsion. The first of these themes is an interest in developing measurement techniques for new spectral territory. Much of the optical-diagnostics effort to date has involved laser sources and measurement schemes that operate in the ultraviolet, visible, and near-infrared spectral regimes. While a wealth of information could be obtained through measurements in the mid- and far-infrared regions, suitable coherent radiation sources have been largely unavailable. The second theme addresses the critical need for techniques that exploit the often-limited optical access afforded by real combustion and propulsion systems. Optical approaches based on coherent-beam techniques and line-of-sight absorption represent potential solutions to these challenges. Transmission characteristics of terahertz radiation suggest the possibility of dealing with optical-access issues through the use of windowless combustors. The third theme concerns the timescales associated with important combustion phenomena and the transient nature of many related events such as ignition, detonation, and extinction. Capturing and describing these processes adequately demands high-speed data acquisition and imaging capability.

Mid-Infrared Measurements with an Optical Parametric Oscillator

Although we continue to develop and apply laser-based combustion diagnostics in the visible and ultraviolet regions of the spectrum, measurements at longer wavelengths offer the potential to overcome several issues encountered when using shorter-wavelength lasers. Many species of interest do not possess electronic transitions for detection using techniques such as laser-induced fluorescence; however, all molecules exhibit vibrational spectra that can be accessed at longer wavelengths. Ultraviolet and visible light are more susceptible to beam steering than infrared radiation is. Particulates can cause large scattering losses in laser radiation during transmission through combustors. Photolytic production of excited species when ultraviolet and visible lasers are used can lead to emission of light that interferes with desired signals. These and other reasons have motivated considerable effort to develop combustion diagnostic techniques for application in the near- and mid-infrared spectral regions.[2-13]

While infrared measurements afford many potential advantages, one significant disadvantage is the relative oscillator strengths for infrared (vibrational) transitions as compared to electronic transitions in the ultraviolet and visible. This situation often limits infrared measurements to path-averaged, line-of-sight absorption applications. Much of the development effort surrounding infrared combustion diagnostics has been targeted at overcoming these limitations through

the use of innovative signal processing schemes such as wavelength multiplexing and derivative spectroscopies. Efforts to extend the effective pathlength over which such measurements are achieved have also served to improve the performance of infrared diagnostics. Other substantial efforts have targeted the development and application of new laser sources designed to excite fundamental transitions in the mid-infrared rather than weaker overtones in the near-infrared.

For much of the history of this relatively new field, communications-grade diode lasers operating in the near infrared were the devices of choice for combustion applications. The demands placed on these systems by the telecommunications industry, in terms of size, weight, robustness, and cost, made them ideally suited for combustion applications, particularly those associated with engineering test facilities or on-board diagnosis, monitoring, and control. These continuous-wave sources also provide high-data-acquisition bandwidth while permitting the ease and flexibility of use achievable through fiber coupling. Perhaps one of the very best demonstrations of the potential utility of diode-laser-based combustion control was achieved with this type of hardware.[7]

While lead-salt diode lasers have provided access to the stronger transitions characteristic of the mid-infrared region for quite some time now, the cyrogenic-cooling requirements of this class of lasers has limited their applicability for combustion measurements, particularly those designed for applications outside the laboratory. Only recently, exciting new developments with quantum-cascade lasers and solid-state optical parametric oscillators (OPO) based on periodically poled lithium niobate (PPLN) have permitted researchers to begin exploiting the potential measurement advantages of the mid-infrared region.

Working closely with laser scientists in the Air Force Research Laboratory's Sensors Directorate and the creative development team at Aculight Corporation, our research group has been pursuing the development and application of an ultranarrowband, doubly resonant, all-solid-state OPO for combustion-diagnostics applications. An OPO is a relatively straightforward nonlinear optical device in which an input or pump wave is split into two output waves, termed the signal and the idler, subject to the criterion $\omega_{pump} = \omega_{signal} + \omega_{idler}$. In other words, the energies of the two output photons sum to the energy of the input photon under all operational conditions. Through suitable manipulation of the non-linear optical material in which the parametric process takes place, the wavelengths of the signal and idler beams can be scanned over spectral regions of interest.

While most OPO's are designed to oscillate on either the signal or the idler beam, the Aculight device is a doubly resonant OPO in which both the signal and the idler oscillate simultaneously in the optical cavity. While this doubly resonant condition is more demanding, it serves to reduce the lasing threshold of the device significantly, thereby permitting the use of a relatively low-power pump source, in this case a single-mode diode laser of the distributed-Bragg-reflector design providing up to 150 mW at 850 nm. Parametric generation of the signal and idler waves occurs in a non-linear PPLN crystal. PPLN provides some important phase-matching characteristics that permit the efficient generation of signal and idler beams over relatively broad tuning ranges through simple temperature tuning of the PPLN crystal. Aside from the pump source and the PPLN crystal, the optical device involves little more than a handful of optical components for pump isolation, beam shaping, and routing. A photograph of two breadboarded systems is provided in Fig. 2, and a schematic diagram of the OPO is depicted in Fig. 3.

The optical design of the Aculight OPO is rather simple, but the control scheme required to provide stable, single-longitudinal-mode operation over long periods of time, to yield coarse tuning over broad spectral regions, and to permit high-frequency wavelength modulation over narrow spectral regions is rather complex. A schematic representation of the control system is depicted in Fig. 4. This system provides simultaneous adjustments to PPLN temperature, diode temperature, diode frequency (current), and OPO cavity length (PZT voltage) during OPO operation. With this control-system engaged, the OPO has remained locked without mode hops for periods exceeding 1.5 hours. Standard deviation in OPO amplitude has been observed to be as low as 0.2% over 35-min periods.

Several systems are responsible for tuning the OPO output over spectral regions of interest. Coarse tuning over broad regions is limited by the poling period of the PPLN crystal and by the optical characteristics of the cavity-optics coatings. Within the tuning curve afforded by a particular crystal-poling period and cavity-optics set, coarse tuning is achieved through adjustments to the PPLN temperature. Fine, continuous tuning of a single longitudinal mode is performed via current tuning of the pump (diode) laser. Feedback-controlled changes to the PZT voltage adjust the cavity length to maintain servo-lock during continuous tuning. A graph describing idler tuning achieved with three different sets of cavity optics is provided in Fig. 5.

The team at Aculight was highly successful in achieving the goals they set forth for this development

effort. Those goals and the actual OPO performance observed are summarized in Table 1. To demonstrate the potential combustion-diagnostics utility of this novel device, the OPO was applied to simple absorption measurements of carbon monoxide (CO) in a gas cell. A single-pass frequency scan through a CO absorption feature at ~2.3 μm is depicted in Fig. 6. These developments indicate the potential of the Aculight OPO and similar devices as room-temperature, low-cost, compact mid-infrared sources with numerous spectroscopic and species-detection applications. Continuing developments of this technology are aimed at achieving kHz frequency modulation, 100-GHz continuous tuning, and locking of the output frequency to atmospheric absorption features. Additional efforts are aimed at moving from the breadboarded device to a brassboard or monolithic configuration that features the robustness, size, weight, and cost necessary for pursuing test-facility and on-board applications.

Far-Infrared Measurements with Terahertz Radiation

In addition to spectral regimes covered by the doubly-resonant OPO, we have pursued measurements at even longer wavelengths using terahertz-based ("T-Ray") technology. Terahertz radiation falls energetically between the far-infrared and microwave spectral regions. While some basic spectroscopy has been achieved at terahertz frequencies in the past using evacuated far-infrared instruments or microwave devices, this region remains a largely "undiscovered" spectral territory dominated by molecular rotational transitions; however, that territory is being rapidly developed as an explosion of new terahertz-radiation research is fueled by the availability of coherent sources and time-gated detection techniques.[14,15]

Much of the excitement over terahertz radiation stems from the transmission characteristics of T-rays that permit the non-destructive evaluation of myriad opaque samples. Novel applications of this technology include examining circuit traces/interconnects inside integrated circuits, detecting tooth decay, locating watermarks in currency, reading text inside envelopes or beneath paint, counting almonds in packaged Hershey bars, and identifying raisins in cereal boxes. Future applications include inspecting luggage, detecting subsurface rust, assessing burned flesh and other damaged tissues, and even seeing through clothing.

In addition to these terahertz-imaging applications, T-rays have been employed to perform basic spectroscopic studies of many neat liquid solvents, both polar and non-polar.[16-19] Terahertz absorption spectroscopy has been applied to gas analysis as well. Static analytes studied to date include hydrogen sulfide[20] and the methyl halides (fluoride, chloride, and bromide).[21-23] Grischkowsky and co-workers have moved beyond studies of static gas samples to the first combustion applications of T-ray technology.[24,25] Line-of-sight-averaged absorption spectra accomplished in a propane-fueled burner reveal terahertz features arising due to high-temperature water molecules. Maxwell-Boltzmann analysis of these data provide flame temperatures.

The potential advantages of T-ray technology over measurements in the visible and ultraviolet regions of the spectrum are similar to those cited above for diagnostics based on near- and mid-infrared radiation. Many species of interest do not possess electronic transitions suitable for detection using techniques such as laser-induced fluorescence; however, many molecules of interest do posses suitable rotational transitions in the terahetz region. As compared to the ultraviolet and the visible, effects due to scattering, optical thickness, and beam steering are typically reduced in the far-infrared due to the wavelength dependence of scattering cross sections and the characteristics of the real and imaginary components of the wavelength-dependent refractive index. Indeed, combustor flowfields that are nearly opaque in the visible region of the spectrum may transmit sufficient terahertz radiation from a coherent source to permit detection and analysis. Our preliminary studies reveal that soot and liquid fuels (JP-8 and JP-8+100 aviation fuels, for example) are largely transparent in the terahertz spectral region. These observations suggest the possible utility of T-ray technology in real-world combustors that exhibit high pressures, significant optical depth, fuel droplets and sprays, and potentially substantial soot loadings.

T-rays may also represent a solution to many optical access and geometric constraints imposed by real-world propulsion systems. Many production combustors are not easily modified for access to detection techniques based on visible or ultraviolet radiation. Even when such modifications are possible, complicated geometries can make analysis of visible signals difficult. For example, the results of a ray-trace computation through the quartz piston bowl of an internal combustion engine under study at Sandia National Laboratories are presented in Fig. 7. Here, a point source emits visible light rays that are then transmitted through the optical piston. Because of the complex geometry, careful attention must be given to multiple image formation and distortion when reducing data acquired using conventional optical techniques. Transmission of signals in the terahertz region of the

spectrum may require a less painstaking evaluation. Advantageous transmission characteristics driving the many imaging applications cited above are attractive features for performing combustion measurements as well. Many solid materials that are opaque in the ultraviolet, visible, or near-infrared regions of the spectrum exhibit transparent bands at frequencies near one terahertz.[26,27] This information suggests that it may be possible to study certain "windowless" combustors without installing glass, quartz, or sapphire windows when using terahertz radiation.

To explore the potential diagnostics utility of T-ray technology while building on Grischkowsky's pioneering combustion work, we recently teamed with Picometrix, Inc., and Innovative Scientific Solutions, Inc. The general features of the terahertz time-domain-spectroscopy (THz-TDS) system Picometrix designed and constructed for our combustion and fuels studies are captured in the schematic diagram in Fig. 8. Terahertz-radiation generation and detection are both accomplished through the interaction of an ultrashort, femtosecond laser pulse with antennas based on silicon or low-temperature-grown GaAs and configured as T-ray transmitters and receivers. THz-TDS is accomplished through the use of pump-probe and Fourier-transform spectroscopic techniques. Typically a single femtosecond laser pulse is split with half the energy directed to the transmitter and the remaining half directed to the receiver. At the transmitter, the femtosecond laser pulse impinges on the semiconductor antenna, liberating short-lived charge carriers that move in the presence of an applied bias potential. It is the motion of these carriers in the bias field that produces the terahertz radiation. This radiation is collected, collimated, and routed to the sample under study. Transmitted T-rays are directed to the receiver substrate. The arrival of these transmitted rays is synchronized with the second half of the femtosecond pulse through optical delay of that laser pulse. The charge carriers liberated when this pulse arrives at the receiver move in the field produced by the transmitted T-rays. Non-destructive detection of this T-ray field is achieved by monitoring the current generated by the motion of these charge carriers. Time-gated detection provides the sensitivity necessary to capture weak T-ray signals.

In practice, measurement of a terahertz absorption spectrum begins with acquisition of terahertz signals in the time-domain. The sequence of events described above is repeated again and again at increasing time delays between the two halves of the laser pulse. A time-resolved terahertz signal is built up one laser pulse at a time by utilizing the phase walkout achieved in conventional pump-probe spectroscopy. The optical delay is swept through the complete terahertz signal, which is typically tens of picoseconds in duration. The time-domain signal is processed via Fourier transformation to yield the frequency-domain absorption information.

The time required to sweep the optical delay through the terahertz waveform defines the available data-acquisition bandwidth. While opto-mechanical delay lines are traditionally employed in such circumstances, we introduced our optical delay through asynchronous optical sampling (ASOPS) techniques.[28-31] This approach utilizes two modelocked femtosecond lasers in place of the single laser employed in conventional pump-probe approaches. By adjusting the two lasers to operate at slightly different repetition rates, a repetitive controlled phase walkout between the two lasers is achieved. The approach represents a no-moving-parts optical delay line capable of achieving much higher sweep rates than those associated with opto-mechanical systems. The details of our THz ASOPS experiments will be the subject of a forthcoming paper.

Time-domain terahertz signals and the corresponding T-ray source spectra obtained by Fourier transformation are depicted in Fig. 9. These data were acquired at ASOPS beat frequencies of 62 and 290 Hz. (The ASOPS beat frequency describes the rate at which the optical delay is swept through the full free temporal range defined by the nominal laser repetition rate. In this case, the delay between the pulses is swept from zero to twelve nanoseconds at the rates identified above.) These signals were acquired for T-ray transmission through room air. Measurements achieved in polar and non-polar liquid solvents (toluene and cyclohexane, respectively) are presented in Fig. 10. Transmission and absorption spectra obtained in room air and a hydrogen-fueled Hencken flame are depicted in Fig. 11. These data reveal water's strong terahertz absorption features. The transmission spectrum obtained through a ceramic liner (Fig. 12) supports the potential for terahertz combustion measurements in windowless combustors. Extensive signal averaging over the course of many seconds was required to achieve the signals depicted in these figures. Since this signal averaging impacts data-acquisition rates, ongoing efforts are devoted to improving sensitivity and system bandwidth.

While the ultrafast lasers that power our THz-TDS system are substantial pieces of hardware in terms of size, weight, and expense, the T-ray modules themselves are actually very compact, light, and robust. The Picometrix team is pursuing numerous continuing developments that promise to reduce the size and cost of the T-ray system while enhancing its potential

diagnostic utility. For their efforts, Picometrix was recently awarded a 2000 R&D 100 Award.

High-Speed Digital Imaging

Experimental and computational techniques for the visualization of fluid flows have emerged as essential tools for increasing our understanding of the physics and chemistry of these flows. Indeed, many—if not most—of the breakthroughs in fluid mechanics and dynamics can be attributed to the understanding achieved through imaging of the various multidimensional structures in fluid flow. The diagrams in Figure 13 capture two methodologies that can be applied to the acquisition of experimental flow-visualization data. In both cases, the goal is to resolve the temporal and spatial scales required to achieve an understanding of the flowfield. These diagrams represent scenarios in which an optical excitation source and detector are employed to capture the dynamics associated with the flowfield. In many instances, no excitation source is required, and the flow is imaged directly using an appropriate detector; however, such instances are not the focus of the current work. Rather this paper addresses those cases where optical excitation is applied to produce the flowfield signal for subsequent detection.

In the first case, the time-evolving dynamics characteristic of the flowfield are explored through careful control of the relative phase between excitation/detection and the fluid-dynamic event. This approach, which is often referred to as phase-locked imaging, relies upon the reproducibility of the phenomena. Time-evolving data are obtained by repeating an experiment many times while incrementing the phase delay between the excitation/detection and fluid-dynamic events in a controlled fashion with each new experiment. In this manner, a sequence of images is constructed over time, and each image represents the features of the flowfield at a precise phase delay. Through post processing, the sequence of images can be joined to produce an animation or movie that reveals the phase-resolved—and, therefore, time-resolved—behavior of the flowfield. This phase-locked approach demands that the fluid dynamics occur in each experiment with a very high degree of reproducibility. Any differences in these events from experiment to experiment will be realized as random, uncorrelated structures in the final phase-resolved animation. Because of this reproducibility requirement, externally driven or forced flows and naturally periodic flows are those most often studied via phase-locked imaging techniques.

While phase-locked imaging has been used extensively to reveal the detailed time dynamics of many interesting flows, these techniques cannot be applied to many important flows that lack the required periodic characteristics and phase-resolved reproducibility. These flows involve fluid dynamics that are truly transient in nature, occurring only once or occurring repeatedly with decidedly different time-evolving structures in each instance. A partial list of such phenomena includes fully developed turbulence, ignition and extinction of combusting flowfields, and detonation events. Studying the time dynamics of these important flowfields requires a visualization approach that can capture an entire sequence of time-resolved images on the time scale of the event under study (i.e., in real time). Such an approach places demanding requirements on the imaging hardware and software employed. Experimental tools must provide sufficient bandwidth to resolve the temporal evolution of the structures of interest. Furthermore, the excitation source and the detector must supply sufficient spectral brightness (in the case of the source) and sensitivity (in the case of the detector) to record the signals of interest in a single pass, given that signal-to-noise enhancement through repetitive sampling is not possible for these types of flowfield studies.

In this section, recent experiments performed through ultrafast real-time imaging are described. The real-time behavior of a gas turbine spark igniter has been explored through the use of a high-repetition-rate laser source and an ultrafast-framing camera. The design of these experiments and the data obtained are presented as examples of the ultrafast real-time imaging methodology. Future experiments are proposed in which simultaneous quantitative concentration measurements are obtained at high repetition rates. We begin by presenting a review of selected high-speed imaging and concentration measurements in combustion.

Background

High-repetition-rate imaging is necessary to study a variety of important combustion processes, and high-speed-imaging demonstrations have been performed for many decades using film to collect images. Equivalent high-speed imaging based on CCD technology has only recently become available, leading to numerous intriguing demonstrations. At the same time, advances in high-repetition rate, short-pulse lasers have led to numerous potential imaging and quantitative point-measurement possibilities.

Ultrafast Imaging. While a variety of probes are available to characterize combustor behavior at high repetition rates, such as high-speed pressure

transducers, it has been demonstrated that photographic records are often superior for investigating combustion processes such as ignition and early flame development.[32] High-speed imaging has been applied to spark-ignition combustion research over much of the 20th Century, with film being used to record images before the advent of digital technology.[33] A film camera operating at 40,000 frames per second—receiving U. S. Patent No. 2,400,885 in 1946—was developed in 1936. Because this camera was found to be too slow for studying engine knock, an ultra-high speed film camera—receiving U. S. Patent No. 2,400,887 in 1946—was developed and applied successfully at rates as high as 200,000 frames per second in 1941. During studies reported in subsequent years, various types of film technology were employed to achieve rates as high as 500,000 frames per second.[34,35]

While high-repetition-rate imaging studies of combustion processes have been accomplished using both natural and chemically induced flame luminosity, both methods are restricted severely in temporal resolution; schlieren and shadowgraph techniques using laser illumination can overcome this difficulty.[36] Lasers offer high irradiance with short temporal pulse durations, important for "freezing" combustion events in time. Suitable pulse-repetition rates can be provided by continuous-wave lasers strobed using an acousto-optic modulator or by mode-locked, continous-wave sources.[36,37] Unfortunately, imaging of schlieren signals to obtain two-dimensional flame shapes has been of limited utility in and of itself, because relating the images obtained to quantities such as temperature, pressure, or concentration is difficult.[38] As a result, high-speed schlieren is often accomplished simultaneously with some quantitative measurement, either globally (as in high-speed pressure-transducer measurements) or locally (as in high-speed LDV measurements of velocity).[36,38]

Simultaneous accomplishment of high-speed schlieren with a second quantitative measurement is complicated when using conventional film to collect signals by synchronization difficulties resulting in temporal uncertainty.[32] Other practical issues include film heating and the handling requirements imposed by large numbers of exposed film reels. Recent advances in digital imaging enable synchronization to other measurement techniques using TTL or ECL signals, and images can be reduced using desktop computers, with the equivalent of miles of film stored on small computer storage disks.

The tools for achieving ultrafrast real-time imaging with the bandwidth required to resolve fluid-dynamic timescales of interest have been difficult to develop and acquire. Ultrafast real-time imaging methodologies have evolved continuously with the development of increasingly capable hardware and software that yield higher repetition rates for excitation and increased data-acquisition bandwidths and storage capability. Improvements in digital-imaging bandwidth have resulted in a number of intriguing demonstrations.

Hanson and coworkers have exploited the latest available technology to achieve time-evolving two-dimensional visualization of important flowfields as well as three-dimensional realizations of complex flows.[39-42] In early work, the Stanford team accomplished instantaneous three-dimensional visualization of combusting flowfields by sweeping a single high-energy laser sheet through the flow using a scanning mirror and capturing a sequence of planar slices using a fast-framing camera system. Laser excitation was provided by a single 1.5-2-μs-wide pulse from a Candela SLL-8000 coaxial flashlamp-pumped dye laser. Pulse energies from 1-5 J were achieved with Rhodamine 590 laser dye. Images of the laser profile as well as planar Mie scattering from soot particles were achieved using a camera system based on the Hadland 790 Imacon image converter that frames at 10 MHz. Sequences of eight to twenty images were generated by the Imacon phosphor and subsequently recorded using photographic film or a CCD camera. By frequency doubling the dye-laser output to 285 nm, pulse energies of 300 mJ/pulse were available for planar laser-induced fluorescence (PLIF) imaging of acetone-seeded flows.

Fansler, French and Drake (1995) captured Mie scattering signals produced using a sheet of light from a copper vapor laser with 30-ns pulses of 2-3 mJ.[43] The scattering signal was collected using a Kodak EktaPro image-intensified high-speed video camera, synchronized to the laser with one pulse per frame at a rate of 4000 frames per second. Images were acquired in a direct-injection engine simultaneously with cylinder pressure measurements and OH-luminousity collected through 10-nm bandpass filters in front of a video camera.

More recently, Ben-Yakar and Hanson have developed an ultra-high-speed schlieren system to study cavity flameholders for ignition and flame stabilization in scramjets.[44] Signals are generated using a Hadland Model 20/50 xenon flashlamp that provides a 200-μs excitation pulse. Schlieren images are recorded using a Hadland Imacon 468 digital camera. This camera employs a beamsplitter to direct the input signal to eight separate 576x384-pixel intensified CCD arrays. Interframing times as short as 10 ns can be achieved with this system.

Long and coworkers explored high-speed digital imaging of turbulent flows, recording time-evolving digital images of gas concentrations and instantaneous three-dimensional fuel-concentration profiles with Mie scattering and biacetyl-fluorescence techniques.[45-47] Excitation sources included an acousto-optically modulated argon-ion laser and a 6-kHz-pulsed copper-vapor laser; detectors included a silicon-intensified target (SIT) vidicon, a Reticon MC9128 photodiode array, and a Spin Physics SP2000 high-speed video recording system.

Lempert, Wu, and Miles recently developed a megahertz-rate, pulse-burst laser system based on Nd:YAG technology that is designed to deliver bursts of pulses at 532 nm with pulse durations between 10 and 100 ns, interpulse periods as short as 1 μs, and pulse energies up to 1 mJ.[48,49] This excitation source is complemented by a Princeton Scientific Instruments (PSI) ultrafast-framing camera designed to accomplish the acquisition of 30 frames of data at framing rates up to 1 MHz. (A second-generation PSI device described below was utilized in the spark-ignition studies that are the subject of the current section of this paper.) This laser and camera have been employed to study supersonic shock-wave/boundary-layer interactions through images obtained via filtered Rayleigh scattering.

At the Lund Institute of Technology, Kaminski and coworkers have accomplished high-speed visualization of spark ignition through the use of a Q-switched Nd:YAG-based laser source and the Hadland eight-frame camera described above.[50] The outputs of four double-pulsed Q-switched lasers are doubled to 532 nm and beam combined to pump a single dye laser and yield a frequency-tunable burst of eight laser pulses. The effects of turbulence on spark-kernel evolution have been explored with these instruments through PLIF measurements.

Spark Ignition. Spark ignition is used widely in the start up of gas-turbine combustors and internal-combustion engines.[51-54] Spark igniters are responsible for initiating the combustion process that sustains engine operation. Demanding applications such as cold start and high-altitude relight require continued enhancement of gas-turbine ignition systems. In automotive systems, spark ignition takes place via three modes known as the breakdown, arc, and glow modes. Breakdown occurs as a spark forms along the discharge path between the electrodes over the course of a few ns. The high-power input creates a shock wave, shaping a high-temperature plasma. This is followed by the arc mode, in which a spark kernel develops over a few μs. These timescales demonstrate the need for extreme temporal resolution in studies of spark ignition.

The behavior of a spark igniter represents an ideal case study for demonstrating ultrafast real-time imaging. Our experiments have been designed to exploit laser schlieren for visualizing refractive-index gradients in the flowfield produced during firing of the spark igniter. These simple schlieren experiments are straightforward to implement and require only a high-repetition-rate laser source for generation of the signal. The spatial variation in spark location from event to event limits the applicability of techniques that utilize a two-dimensional light sheet for illumination. Schlieren yields a line-of-sight image that captures the spark despite variations in position and morphology. Furthermore, the spark characteristics are of great practical interest. Concerns over engine cold start and high-altitude relight are driving the enhancement of traditional spark-based systems and development of new ignition systems that incorporate lasers and microwave plasmas, for example. Through continuing laboratory experiments, the ultrafast real-time imaging techniques described in this paper are currently being applied to the characterization and improvement of the spark-ignition process.

Quantitative High-Repetition-Rate Concentration Measurements at a Point. The potential for coupling high-speed imaging with quantitative point measurements has been enhanced by the advent of tunable, high-repetition-rate laser sources based on Ti:sapphire. These lasers produce pulses at rates up to 100 MHz, enabling synchronization with the fastest cameras available. Various amplification techniques have been developed to provide increased pulse energy at reduced repetition rates. Pulse-selection devices enable practical synchronization with high-speed cameras.

These lasers are easily adjusted to yield output pulsewidths from tens of fs to hundreds of ps. This flexibility suggests a variety of potential schemes for obtaining quantitative point measurements of concentration with extreme data-acquisition bandwidth.[55-60]

Experimental Procedure

Gas Turbine Spark Igniter. Spark events produced by a Unison Industries Vision spark-ignition system were visualized using the ultrafast real-time imaging system described in detail below. The Vision system, which is utilized in both military and commercial aviation, is designed to produce a tailored ignition spark at the tip of the igniter plug through delivery of a pulse (nominal energy 4-12 J) from the Vision-system igniter box. The plug tip is composed of a ring electrode encompassing a center electrode. Upon delivery of the igniter-box pulse, an arc occurs across the center-electrode/ring-

electrode gap. Because the location and physical characteristics (morphology, etc.) of this arc can vary from shot to shot, an ultrafast real-time imaging system is required to capture the detailed time-dynamics of the process. If the spark event were highly reproducible from shot to shot, phase-locked imaging could be applied rather than the real-time approach.

High-Repetition-Rate Sources. Laser schlieren techniques were employed to visualize propagation of the shock produced during firing of the Unison Industries Vision-system spark igniter. The characteristics of the spark event demand high temporal resolution and ultrafast real-time imaging for capture of the physics of interest. To accomplish the required temporal resolution, two different high-repetition-rate laser sources were considered. The first is the Spectra-Physics "Merlin" intracavity-frequency-doubled Nd:YLF laser, and the second is the Spectra-Physics "Tsunami" modelocked Ti:sapphire laser.

The Merlin is a Q-switched Nd:YLF laser that operates at kilohertz repetition rates. The device installed at Wright-Patterson Air Force Base is configured for 50-kHz operation and produces a 13-W pulsetrain (260 μJ/pulse) at 527 nm through intracavity doubling of the Nd:YLF fundamental in lithium triborate (LBO). The multi-mode output beam provides a uniform spatial beam profile ideal for flow-visualization applications. While the Merlin's high spectral brightness and mode characteristics proved to be excellent for studies of the spark igniter, its repetition rate was insufficient for resolving the shock phenomena of interest. This situation motivated a series of studies that employed the pulse-selected Tsunami as an excitation source.

The Tsunami modelocked Ti:sapphire laser employed in these studies is configured to produce an 82-MHz pulsetrain, spectrally tunable over the wavelength range 800-900 nm. Experiments were accomplished at 850 nm for all cases described here. When pumped by the 5-W, 532-nm output of a Spectra-Physics Millennia V intracavity-doubled (LBO) Nd:YVO4 laser, the Tsunami provides ~1 W output power (12 nJ/pulse). The 82-MHz repetition rate is excessive for imaging the spark igniter while using the 1-MHz ultrafast-framing camera described below; therefore, the repetition rate of the laser was reduced using a Spectra-Physics Model 3980 pulse selector. This device employs a TeO_2 acousto-optic modulator to select subsets of pulses from the full 82-MHz output pulsetrain. Losses in the pulse selector reduce the laser energy to 8 nJ/pulse.

Ultrafast-Framing Camera. Laser-schlieren images of the Unison Industries spark igniter were captured using a PSI ultrafast framing camera. This device features a CCD image sensor that can be exposed at rates up to 1 MHz and provides an on-chip storage array for 32 images. The array associated with the camera employed in these experiments is 180x90 pixels.

Synchronization and Timing. A number of configurations for ultrafast real-time imaging were explored. Preliminary experiments were designed to capture the spontaneous emission produced during firing of the spark igniter. Synchronization and timing of the various experimental events were achieved easily during these experiments. The camera was configured with an appropriate lens and placed to view the tip of the spark-igniter plug. A photodiode was arranged to collect light from the spark-ignition event. The camera was configured in a pre-trigger mode in which data frames are acquired continuously and processed through the on-chip storage array in a first-in-first-out (FIFO) arrangement. The spark igniter was fired via user-entered commands to a personal computer that was driving the Unison exciter box and the spark plug. The signal produced at the photodiode was employed to trigger the camera, terminating data acquisition in the pre-trigger mode and capturing the spark-igniter-image data in the on-chip storage array.

Laser-based schlieren studies of the spark igniter required a more sophisticated experimental arrangement, with greater attention to the details of synchronization and timing. Three unique strategies for schlieren-data acquisition were explored. In the first approach, the Merlin Q-switched Nd:YLF laser provided light for the schlieren measurements, and the 50-kHz laser served as the master oscillator for the experiment. The ultrafast framing camera was configured in the “multi” external trigger mode, with triggers being supplied by the spark-igniter event and the laser. Under these conditions, 32 frames of camera data were acquired in synchrony with the laser during the 640-μs period spanning the spark event. This approach provided tremendous optical energies and saturating signals at the camera; therefore, neutral-density filters were inserted into the optical path to attenuate the laser beam. Unfortunately, the 50-kHz repetition rate of the laser proved insufficient to resolve the progress of the spark-initiated shock wave adequately.

This situation prompted experiments conducted via a second approach in which the pulse-selected Tsunami Ti:sapphire laser was utilized to produce the schlieren signal. As in the previous experiments, the laser served as the master oscillator, and the camera was slaved to the laser and the spark event via the “multi” external trigger mode. This arrangement permitted the acquisition of image data at framing rates up to 800 kHz, improving the temporal resolution over that

achieved in the Merlin experiments by a factor of sixteen.

The third and final approach, however, produced the best visualization and enabled spark imaging at the full 1-MHz data-acquisition bandwidth of the camera. For these experiments, the camera served as the master oscillator, and the pulse selector—and, therefore, the laser—were slaved to the camera. A block diagram of the experimental apparatus is depicted in Figure 14. The Millennia/Tsunami/pulse selector provide the laser pulse for schlieren measurements. The output pulsetrain is expanded to a nominal diameter of ~32 mm through two 4x telescopes. The collimated, expanded laser beam traverses a sample region in which the spark-igniter plug is suspended. A lens collects the transmitted light, which is focused to a point where a knife edge is inserted. Light traveling past the knife edge is imaged through a neutral-density filter (ND=1) and an interference filter (center frequency=850nm, bandwidth=10 nm) onto an ultrafast-framing camera using a Nikon lens.

Details of the synchronization and timing are presented schematically in Figure 15. The ultrafast framing camera is configured in the post-trigger mode and, therefore, acquires images continuously until a spark event occurs. The spark event is initiated by the experimenter through entry of commands at the personal computer. These commands trigger the Unison exciter box, firing the spark plug and producing a trigger via the remote module that drives a digital delay generator (DDG). This DDG triggers the camera. Once the camera is triggered, it acquires and stores the 32 images that comprise the final data set. Trigger delays are carefully adjusted to ensure that the frames are acquired during the spark event. Once triggered, the camera is responsible for driving the pulse selector and synchronizing the laser with the image-acquisition process. The camera is configured to record images at its full 1-MHz acquisition rate. During each frame, the camera generates a vertical-strobe pulse that drives the pulse selector. This strobe pulse is shaped and further processed with a pulse generator and then mixed with the ~41-MHz signal from the Ti:sapphire modelocker. This process ensures that a single laser pulse is selected from the 82-MHz pulsetrain during the exposure time associated with each of the 32 camera frames. The vertical-strobe-driven pulse generator can be adjusted to select an envelope of pulses from the 82-MHz train during each framing event. For example, experiments were accomplished with 10 and 100 laser pulses per frame; however, the data presented in this paper were achieved with a single pulse for each frame. Those data, depicting the propagation of the spark-initiated shock, are presented in Figure 16.

Conclusions

Ultrafast real-time imaging of the shock structure produced by a Unison Industries spark igniter has been accomplished. Spontaneous-emission and laser-schlieren techniques have been demonstrated in conjunction with a number of high-repetition-rate laser sources (50-kHz, Q-switched Nd:YLF laser; pulse-selected, 82-MHz modelocked Ti:sapphire laser) and an ultrafast-framing CCD camera (framing rates up to 1 MHz). Future efforts will be devoted to relating high-speed-schlieren images to quantitiative point concentration measurements acquired simultaneously.

Summary

Some emerging combustion diagnostics under development at the Air Force Research Laboratory's Propulsion Directorate have been reviewed. These ongoing activities are based on three themes: 1) Extending the spectral bandwidth of radiation sources to longer wavelengths to achieve advantages not possible in other regions of the spectrum; 2) Addressing limited optical access by using line-of-sight absorption or exploiting spectral regions in which combustor materials may become suitably transparent; and 3) Increasing the bandwidth of imaging techniques to enable real-time, digital imaging of ultrafast combustion phenomena. The latest progress has been described for techniques based on doubly resonant OPO's, time-domain terahertz spectroscopy, and ultrafast (up to 1-MHz framing rate) digital imaging with modelocked light sources.

Acknowledgments

The authors gratefully acknowledge the efforts of Keith Grinstead who has contributed greatly to all of the developments described herein. The talented research team at Aculight Corporation (Angus Henderson, Pam Roper, and Roy Mead) are credited with the success of our OPO program. We wish to thank Ken Schepler, George Tietz, and Virginia McMillan (all with the Air Force Research Laboratory's Sensors Directorate) for their invaluable contributions to this effort as well. Mike Brown of Innovative Scientific Solutions, Inc., and the Picometrix research team, including Van Rudd, Dave Zimdars, Matt Warmuth, Steve Williamson, and Rob Risser, are responsible for our achievements with terahertz radiation. High-speed imaging of spark ignition benefited considerably from the talents of collaborators at Unison Industries (Mike Cochran and John Frus).

References

1. A. C. Eckbreth, *Laser Diagnostics for Combustion, Temperature, and Species*, 2nd Edition, Gordon & Breach, 1996.
2. J. Wang, M. Maiorov, J. B. Jeffries, D. Z. Garbuzov, J. C. Connolly, and R. K. Hanson, "A Potential Remote Sensor of CO in Vehicle Eshausts Using 2.3 μm Diode Lasers," Measurement Science & Technology, Vol. 11, No. 11, pp. 1576-1584 (2000).
3. B. J. Kirby and R. K. Hanson, "Planar Laser-Induced Fluorescence Imaging of Carbon Monoxide using Vibrational (Infrared) Transitions," Applied Physics B, Vol. 69, pp. 505-507 (1999).
4. R. M. Mihalcea, M. E. Webber, D. S. Baer, R. K. Hanson, G. S. Feller, W. B. Chapman, "Diode-Laser Absorption Measurements of CO_2, H_2O, N_2O, and NH_3 near 2.0 μm," Applied Physics B, Vol. 67, pp. 283-288 (1998).
5. R. M. Mihalcea, D. S. Baer, and R. K. Hanson, "A Diode-Laser Absorption Sensor System for Combustion Emission Measurements," Measurement Science & Technology, Volume 9, No. 3, pp. 327-338 (1998).
6. D. S. Baer, V. Nagali, E. R. Furlong, R. K. Hanson, and M. E. Newfield, "Scanned- and Fixed-Wavelength Absorption Diagnostics for Combustion Measurements using a Multiplexed Diode-Laser Sensor System," AIAA Journal, Vol. 34, No. 3, 489-493 (1996).
7. E. R. Furlong, D. S. Baer, and R. K. Hanson, "Combustion Control using a Multiplexed Diode-Laser Sensor System," Proceedings of the Combustion Institute, Vol. 26, pp. 2851-2858 (1986).
8. M. G. Allen, "Diode Laser Absorption Sensors for Gas-Dynamic and Combustion Flows," Measurement Science and Technology, Vol. 9, No. 4, pp. 545-562 (1998).
9. D. M. Sonnenfroh and M. G. Allen, "Absorption Measurements of the Second Overtone Band of NO in Ambient and Combustion Gases with a 1.8-μM Room-Temperature Diode Laser," Applied Optics, Vol. 36, No. 30, pp. 7970-7977 (1997).
10. M. F. Miller, W. J. Kessler, and M. G. Allen, "Diode Laser-Based Mass Flux Sensor for Subsonic Aeropropulsion Inlets," Applied Optics, Vol. 35, No. 24, pp. 4905-4912 (1996).
11. J. A. Silver and D. J. Kane, "Diode Laser Measurements of Concentration and Temperature in Microgravity Combustion," Measurement Science & Technology, Vol. 10, No. 10, pp. 845-852 (1999).
12. D. B. Oh, M. E. Paige, and D. S. Bomse, "Frequency Modulation Multiplexing for Simultaneous Detection of Multiple Gases by Use of Wavelength Modulation Spectroscopy with Diode Lasers," Applied Optics, Vol. 37, No. 12, pp. 2499-2501 (1998).
13. J. A. Silver, D. J. Kane, P. S. Greenberg, "Quantitative Species Measurements in Microgravity Flames with Near-IR Diode Lasers," Applied Optics, Vol. 34, No. 15, pp. 2787-2801 (1995).
14. M. C. Nuss and J. Orenstein, "Terahertz Time-Domain Spectroscopy," in *Millimeter and Submillimeter Wave Spectroscopy of Solids*, G. Gruner, Editor, Springer, 1998.
15. An excellent terahertz-radiation tutorial is available at http://elec-engr.okstate.edu/thzlab/, and a long list of links is available at http://www-ece.rice.edu/~daniel/groups.html.
16. J. T. Kindt, and C. A. Schmuttenmaer, "Far-Infrared Dielectric Properties of Polar Liquids Probed by Femtosecond Terahertz Pulse Spectroscopy," Journal of Physical Chemistry A, Vol. 100, No. 24, pp. 10373-10379 (1996).
17. B. N. Flanders, R. A. Cheville, D. Grischkowsky, and N. F. Scherer, "Pulsed Terahertz Transmission Spectroscopy of Liquid $CHCl_3$, CCl_4, and their Mixtures," Journal of Physical Chemistry A, Vol. 100, No. 29, pp. 11824-11835 (1996).
18. L. Thrane, R.H. Jacobsen, P. U. Jepsen, and S. R. Keiding, "THz Reflection Spectroscopy of Liquid Water," Chemical Physics Letters, Vol. 240, p. 330 (1995).
19. J. E. Pederson, and S. R. Keiding, "THz Time-Domain Spectroscopy of Nonpolar Liquids," IEEE Journal of Quantum Electronics, Vol. 28, p. 2518 (1992).
20. G. Mouret, W. Chen, D. Boucher, R. Bocquet, P. Mounaix, and D. Lippens, "Gas Filter Correlation Instrument for Air Monitoring at Submilliter Wavelengths," Optics Letters, Vol. 24, p. 351 (1999).
21. H. Harde, N. Katzenellenbogen, and D. Grischkowsky, "Terahertz Coherent Transients from Methyl Chloride Vapor," Journal of the Optical Society of America B, Vol. 11, p. 1018 (1994).
22. H. Harde, R. A. Cheville, and D. Grischkowsky, "Terahertz Studies of Collision-Broadened Rotational Lines," Journal of Physical Chemistry A, Vol. 101, p. 3646 (1997).

23. H. Harde, N. Katzenellenbogen, and D. Grischkowsky, “Line-Shape Transition of Collision Broadened Lines,” Physical Review Letters, Vol. 74, p. 1307 (1995).
24. R.A. Cheville and D. Grischkowsky, “Observation of Pure Rotational Absorption Spectra in the ν_2 Band of Hot H_2O in Flames," Optics Letters, Vol. 23, pp. 531-533 (1998)
25. R.A. Cheville and D. Grischkowsky, "Far Infrared, THz Time Domain Spectroscopy of Flames," Optics Letters, Vol. 20, pp. 1646-1648 (1995).
26. D. M. Mittleman, M. Gupta, R. Neelamani, R. G. Baraniuk, J. V. Rudd, and M. Koch, “Recent Advances in Terahertz Imaging,” Applied Physics B, Vol. 68, p. 1085 (1999).
27. M. N. Afsar, “Precision Millimeter-Wave Measurements of Complex Refractive Index, Complex Dielectric Permittivity, and Loss Tangent of Common Polymers,” IEEE Transactions on Instrumentation and Measurement, Vol. IM-36, p. 530 (1987).
28. G. J. Fiechtner, G. B. King, and N. M. Laurendeau, “Quantitative Concentration Measurements of Atomic Sodium in an Atmospheric Hydrocarbon Flame with Asynchronous Optical Sampling,” Applied Optics, Vol. 34, p. 1117, (1995).
29. G. J. Fiechtner, G. B. King, N. M. Laurendeau, and F. E. Lytle, “Measurements of Atomic Sodium in Flames by Asynchronous Optical Sampling: Theory and Experiment,” Applied Optics, Vol. 31, p. 2849 (1992).
30. P. A. Elzinga, R. J. Kneisler, F. E. Lytle, Y. Jiang, G. B. King, and N. M. Laurendeau, “Pump/Probe Method for Fast Analysis of Visible Spectral Signatures Utilizing Asynchronous Optical Sampling,” Applied Optics, Vol. 26, p. 4303 (1987).
31. P. A. Elzinga, F. E. Lytle, Y. Jiang, G. B. King, and N. M. Laurendeau, “Pump/Probe Spectroscopy by Asynchronous Optical Sampling,” Applied Spectroscopy, Vol. 41, p. 2 (1987).
32. J. C. Keck, J. B. Heywood, and G. Noske, “Early Flame Development and Burning Rates in Spark Ignition Engines and Their Cyclic Variability,” SAE Paper No. 870164 (1988).
33. C. D. Miller, “Knock as Shown ay Photographs Taken at 40,000 and 200,000 Frames Per Sec,” SAE Quarterly Transactions, Vol. 1, No. 1, pp. 98-143 (1947).
34 T. Male, “Photographs at 500,000 Frames Per Second and Detonation in a Reciprocating Engine,” Proceedings of the Combustion Institute, Vol. 3, pp. 721-726 (1949).
35. C. A. Amann, “Classical Combustion Diagnostics for Engine Research,” SAE Paper No. 850395 (1986).
36. P. O. Witze and T. M. Dyer, “Laser Measurement Techniques Applied to Turbulent Combustion in Piston Engines,” Experiments in Fluids, Vol. 4, pp. 81-92 (1986).
37. G. V. Sklizkov, “Lasers in High-Speed Photography,” in *Laser Handbook*, F. T. Arecchi and E. O. Schulz-Dubois, Editors, Vol. 2, pp. 1545-1577, North-Holland, 1972.
38. U. Spicher, H. Kröger, and J. Ganser, “Detection of Knocking Combustion using Simultaneously High-Speed Schlieren Cinematography and Multi Optical Fiber Technique,” SAE Paper No. 912312 (1991).
39. J. M. Seitzman, B. J. Patrie, P. H. Paul, and R. K. Hanson, “Instantaneous 3-D and Temporal Evolution Measurements by Rapid Acquisition of Planar Images,” AIAA 91-0178 (1991).
40. B. J. Patrie, J. M. Seitzman, and R. K. Hanson, “Planar Imaging at High Framing Rates: System Characterization and Measurements,” AIAA 92-0584 (1992).
41. B. J. Patrie, J. M. Seitzman, and R. K. Hanson, “Planar Imaging for 3-D Flow Visualization,” 22nd International Congress on High Speed Photography and Photonics, SPIE Vol. 1801 (1992).
42. B. J. Patrie, J. M. Seitzman, and R. K. Hanson, “Planar Imaging at High Framing Rates: System Characterization and Measurements, II,” AIAA 93-0364 (1993).
43. T. D. Fansler, D. T. French, and M. C. Drake, “Fuel Distributions in a Firing Direct-Injection Spark-Ignition Engine using Laser-Induced Fluorescence Imaging,” SAE Paper No. 950110 (1995).
44. Ben-Yakar and R. K. Hanson, “Cavity Flameholders for Ignition and Flame Stabilization in Scramjets: Review and Experimental Study,” AIAA 98-3122 (1998).
45. M. Winter, J. K. Lam, and M. B. Long, “Techniques for High-Speed Digital Imaging of Gas Concentrations in Turbulent Flows,” Experiments in Fluids, Vol. 5, pp. 177-183 (1987).
46. M. B. Long and B. Yip, “Measurement of Three-Dimensional Concentrations in Turbulent Jets and Flames,” Proceedings of the Combustion Institute, Vol. 22, pp. 701-709 (1988).
47. B. Yip, R. L. Schmitt, and M. B. Long, “Instantaneous Three Dimensional Concentration Measurments in Turbulent Jets and Flames,” Optics Letters, Vol. 13, pp. 96-98 (1987).

48. W. R. Lempert, P.-F. Wu, B. Zhang, R. B. Miles, J. L. Lowrance, V. Mastrocola, and W. F. Kosonocky, "Pulse-Burst Laser System for High-Speed Flow Diagnostics," AIAA 96-0179 (1996).
49. W. R. Lempert, P.-F. Wu, and R. B. Miles, "Filtered Rayleigh Scattering Measurements Using a MHz Rate Pulse-Burst Laser System," AIAA 97-0500 (1997).
50. C. F. Kaminski, A. Franke, J. Hult, M. Alden, and R. B. Williams, "Applications of a Multiple-Pulse YAG Laser/Framing Camera System for Ultrafast Visualization of Combustion Processes," Work-in-Progress poster presented at the 27th Symposium (International) on Combustion, Boulder (1998).
51. C. F. Daniels and B. M. Scilzo, "The Effects of Electrode Design on Mixture Ignitability," SAE Paper No. 960606 (1996).
52. J. Kim and R. W. Anderson, "Spark Anemometry of Bulk Gas Velocity at the Spark Plug Gap of a Firing Engine," SAE Paper No. 952459 (1995).
53. N. Ozdor, M. Dulger, and E. Sher, "Cyclic Variability in Spark Ignition Engines: A Literature Survey," SAE Paper No. 940987 (1994).
54. G. T. Kalghatgi, "Spark Ignition, Early Flame Development, and Cyclic Variation in I. C. Engines," SAE Paper No. 870163 (1987).
55. W. Renfro, G. B. King and N. M. Laurendeau, "Scalar Time-Series Measurements in Turbulent $CH_4/H_2/N_2$ Nonpremixed Flames: CH," Combustion and Flame, Vol. 122, pp. 139-150 (2000).
56. M. W. Renfro, Y. R. Sivathanu, J. P. Gore, G. B. King, and N. M. Laurendeau, "Time-Series Analysis and Measurements of Intermediate Species Concentration Spectra in Turbulent Nonpremixed Flames," Proceedings of the Combustion Instititue, Vol. 27, pp. 1015-1022, (1998).
57. M. W. Renfro, S. D. Pack, G. B. King, and N. M. Laurendeau, "Hydroxyl Time-Series Measurements in Laminar and Moderately Turbulent Methane/Air Diffusion Flames," Combustion and Flame, Volume 115, pp. 443-455 (1998).
58. M. W. Renfro, M. S. Klassen, G. B. King, and N. M. Laurendeau, "Time-Series Measurements of CH Concentration in Turbulent CH_4/Air Flames by Use of Picosecond Time-Resolved Laser-Induced Fluorescence," Optics Letters, Vol. 22, No. 3, pp. 175-177 (1997).
59. G. J. Fiechtner and M. A. Linne, "Absolute Concentrations of Potassium by Picosecond Pump/Probe Absorption in Fluctuating, Atmospheric Flames," Combustion Science and Technology, Vol. 100, pp. 11-27 (1994).
60. G. J. Fiechtner, "Quantitative concentration measurements in atmospheric-pressure flames by picosecond pump/probe absorption spectroscopy," Ph.D. Dissertation, Purdue University, West Lafayette, IN (1992).

Parameter	Phase II Goal	Demonstrated
Accessible Wavelength Region	1.1 to 4.0 um	1.1 to 1.4 um, 2.2 to 3.7 um
Output Linewidth	< 5 MHz (< 0.02 pm)	< 3 MHz
Frequency Stability	± 10 MHz (0.04 pm)	± 10 MHz
Amplitude Stability	± 5%	0.2%
Single-Mode Tuning Range	100 GHz	17 GHz (PZT Limited)
Tuning Range	200 nm	250 to 600 nm
Output Power	10 mW	18 mW

Table 1. Design goals and demonstrated performance of the Aculight ultranarrowband, doubly resonant, mid-infrared optical parametric oscillator.

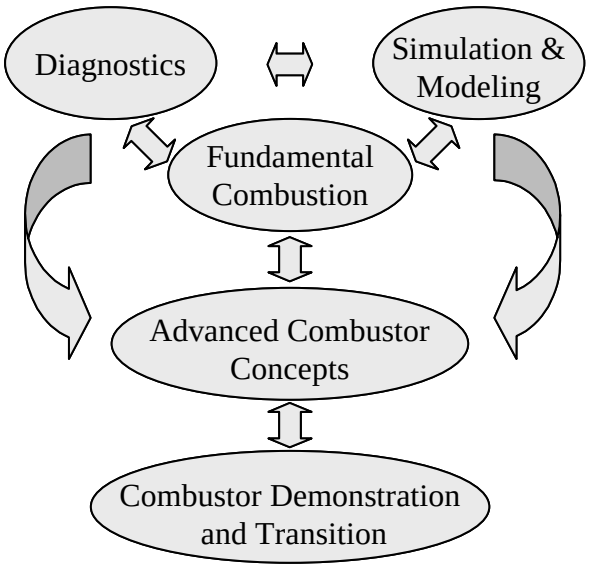

Figure 1. A design philosophy for transitioning basic research activities through exploratory development and applied engineering at AFRL.

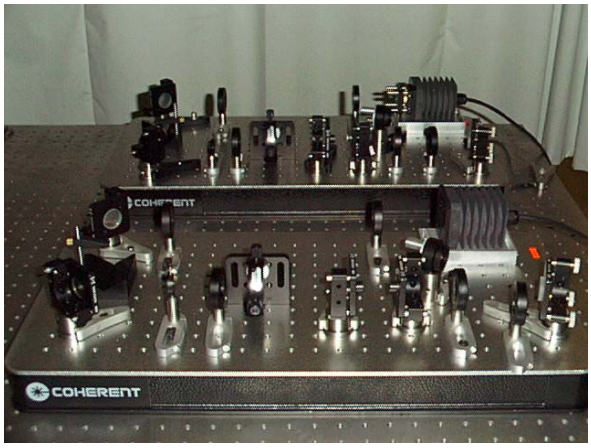

Figure 2. Breadboarded Aculight ultranarrowband, doubly resonant, mid-infrared optical parametric oscillators.

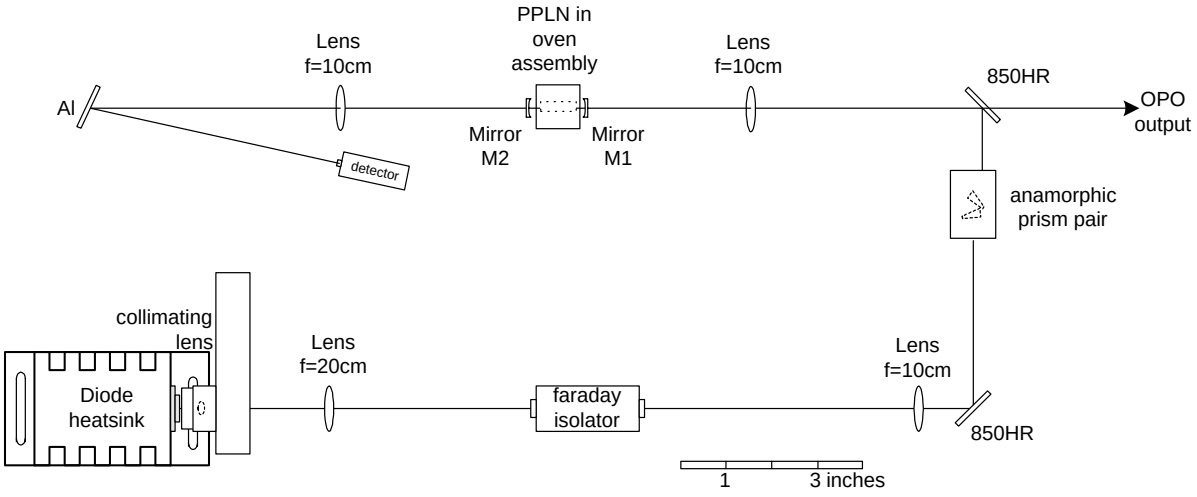

Figure 3. Schematic diagram of the Aculight ultranarrowband, doubly resonant, mid-infrared optical parametric oscillator.

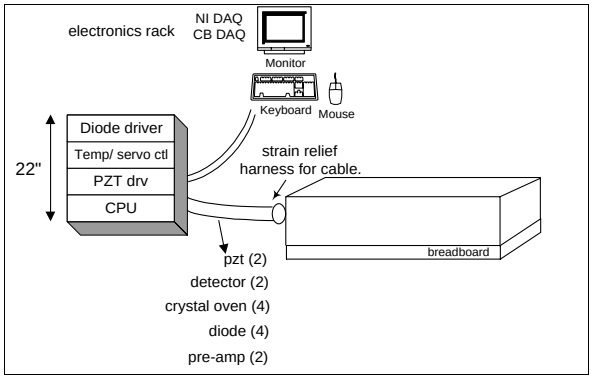

Figure 4. Schematic diagram of the control system for the Aculight ultranarrowband, doubly resonant, mid-infrared optical parametric oscillator.

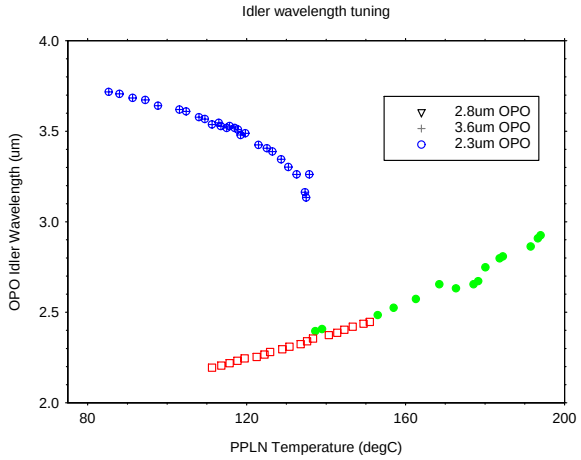

Figure 5. Coarse wavelength tuning achieved for the idler beam of the Aculight ultranarrowband, doubly resonant, mid-infrared optical parametric oscillator.

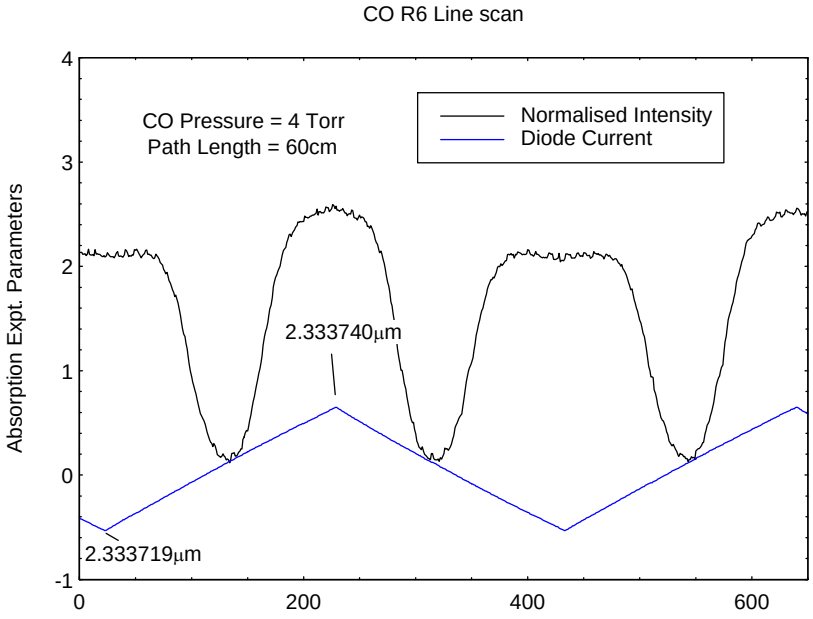

Figure 6. CO line scans achieved with the idler beam of the Aculight ultranarrowband, doubly resonant, mid-infrared optical parametric oscillator.

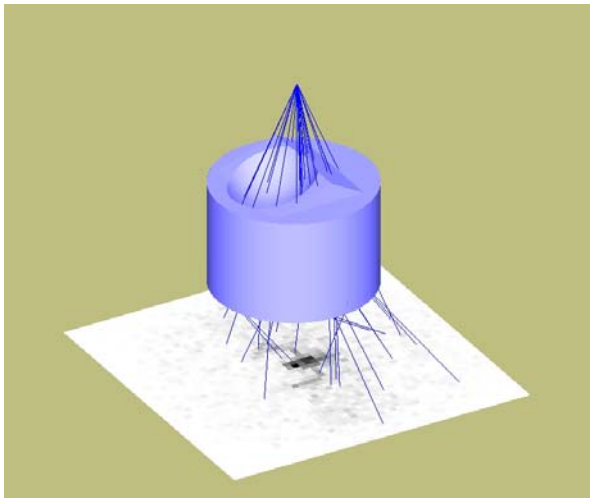

Figure 7. Ray-trace computation through the quartz piston bowl of an internal combustion engine under study at Sandia National Laboratories.

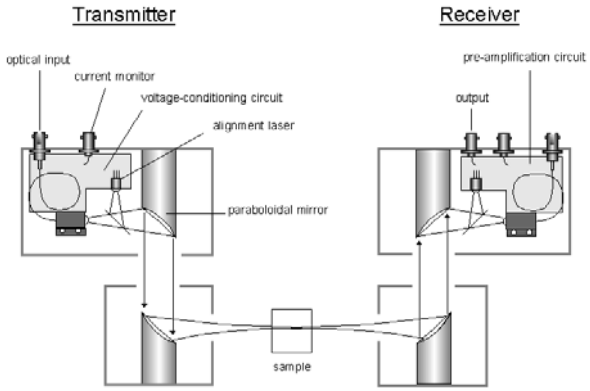

Figure 8. Schematic diagram of a terahertz time-domain-spectroscopy (THz-TDS) system.

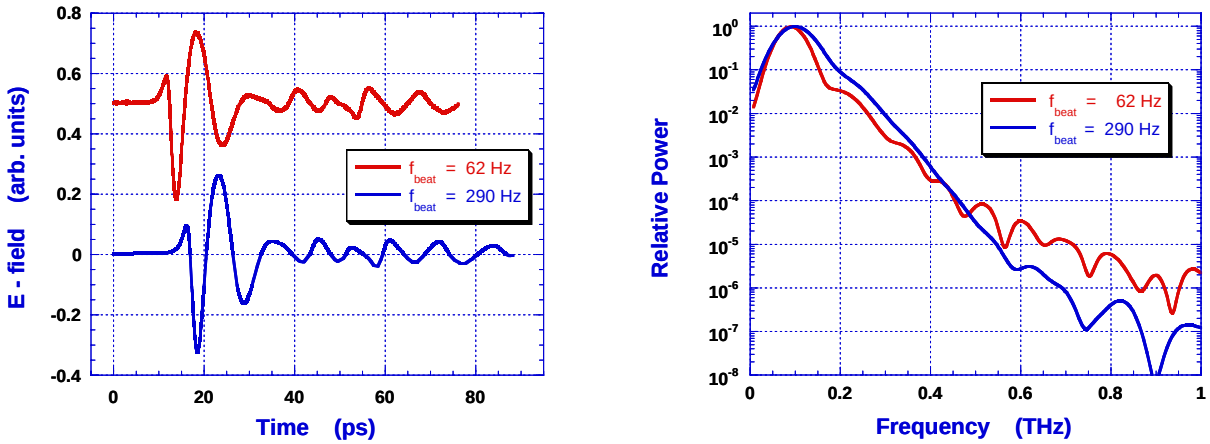

Figure 9. Time and frequency domain representations of the THz-TDS system source spectrum. Data were acquired at ASOPS beat frequencies of 62 and 290 Hz.

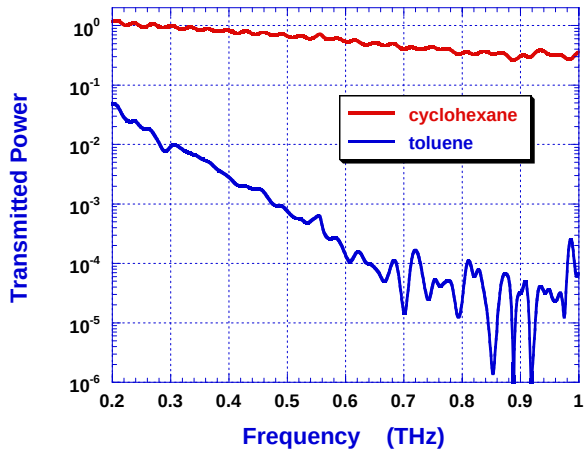

Figure 10. Terahertz transmission spectra for polar (toluene) and non-polar (cyclohexane) neat liquid solvents.

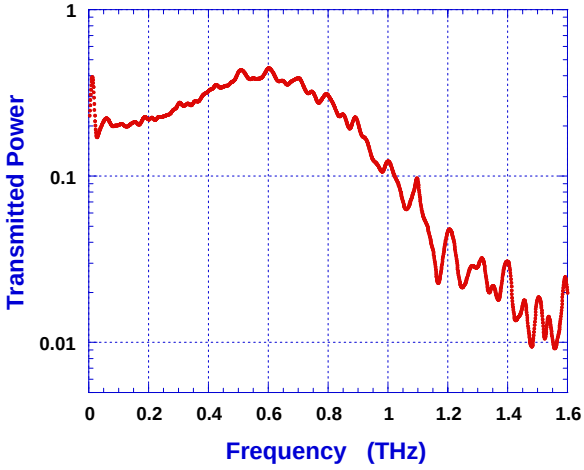

Figure 12. Terahertz transmission spectrum for a ceramic liner that might serve as an element in a windowless combustor design.

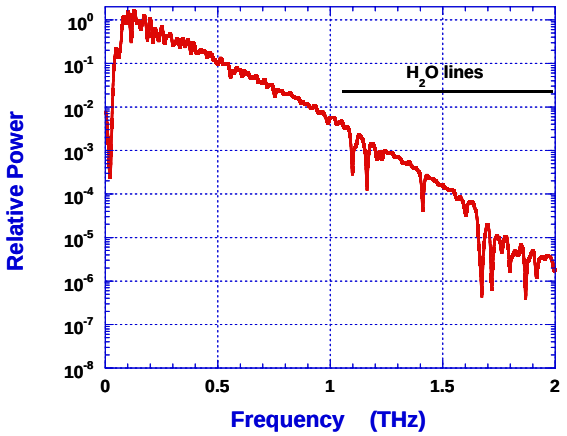

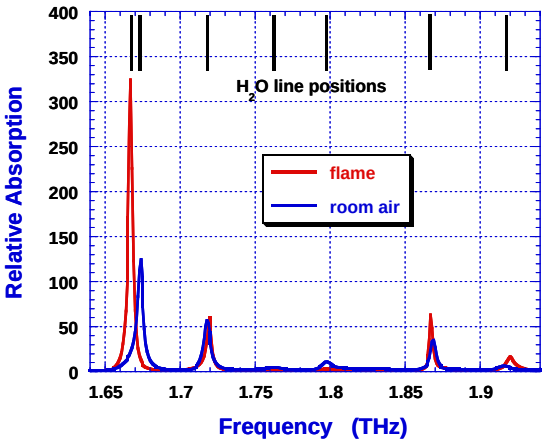

Figure 11. Terahertz spectra obtained in room air and in a hydrogen-fueled Hencken flame.

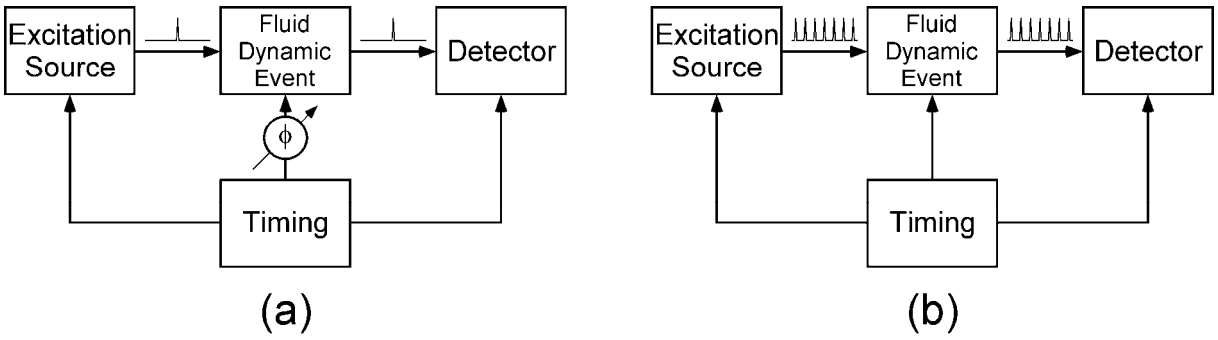

Figure 13. Experimental methodologies for flow visualization. (a) Phase-locked approach in which the excitation and detection events are synchronized in time while the phase of the fluid-dynamic event is varied with respect to excitation/detection. (b) Ultrafast real-time approach in which a high-repetition-rate excitation source and an ultrafast-framing detector are utilized to capture the time dynamics of a single transient fluid-dynamic event.

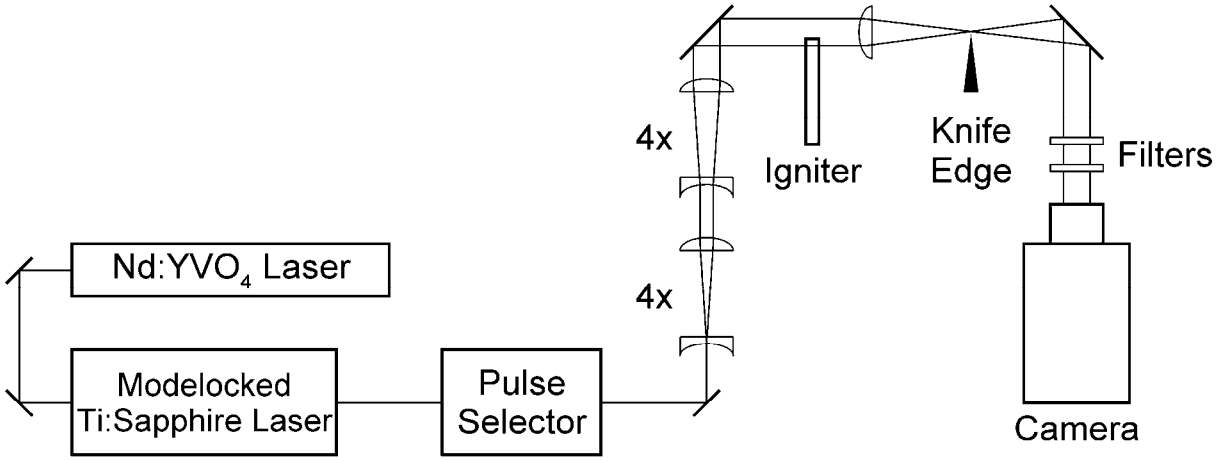

Figure 14. Experimental apparatus for ultrafast real-time laser-schlieren imaging of a Unison Industries spark igniter.

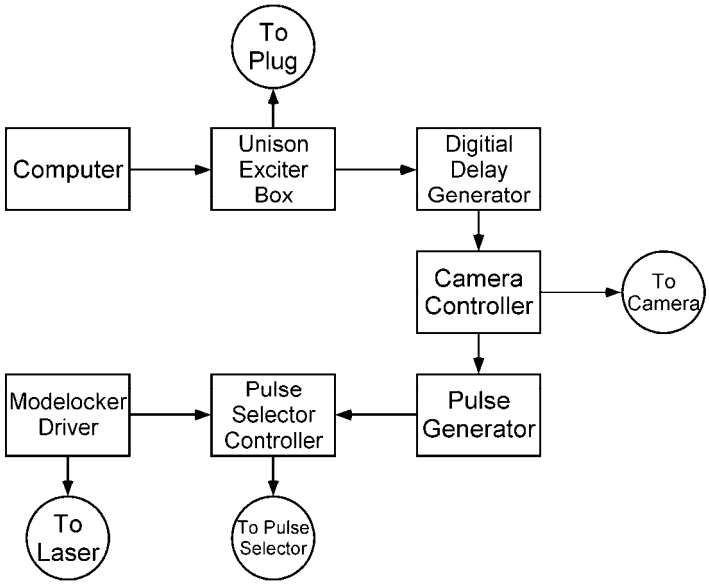

Figure 15. Diagram of electronic timing connections for ultrafast real-time laser-schlieren measurements.

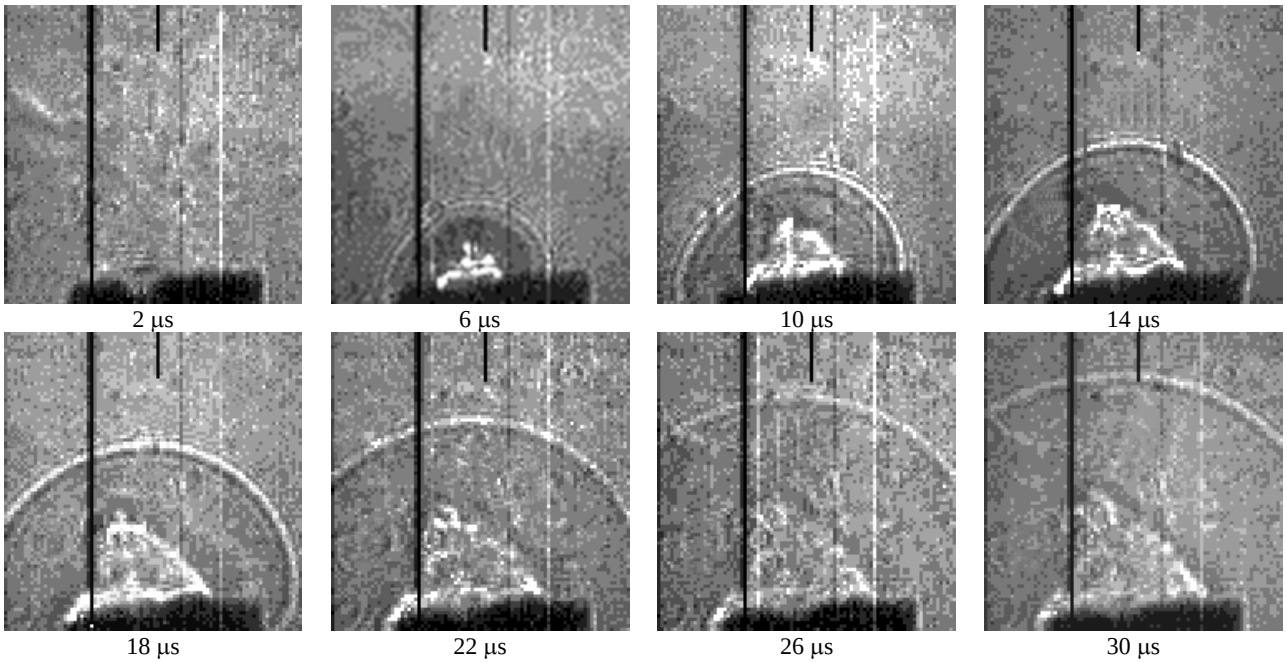

Figure 16. A selection of laser-schlieren images acquired at 1-MHz framing rate that depicts propagation of the shock produced during firing of the Unison Industries spark igniter.

Invited Paper “Optical Turbine-Engine Diagnostics for Ground-Test and On-Board Applications” prepared for the NATO Research & Technology Agency Applied Vehicle Technology Panel Specialists Meeting on Recent Developments in Non-Intrusive Measurement Technology for Military Application on Model and Full-Scale Vehicles (AVT-124), which was held during April 2005 in Budapest, Hungary

Optical Turbine-Engine Diagnostics for Ground-Test and On-Board Applications

James R. Gord
Combustion & Laser Diagnostics Research Complex
Air Force Research Laboratory, Propulsion Directorate
Wright-Patterson AFB OH 45433-7251, USA

james.gord@wpafb.af.mil

Terrence R. Meyer
Innovative Scientific Solutions, Inc.
Dayton OH 45440-3638

terrence.meyer@wpafb.af.mil

Sukesh Roy
Innovative Scientific Solutions, Inc.
Dayton OH 45440-3638

sroy@woh.rr.com

Michael S. Brown
Innovative Scientific Solutions, Inc.
Dayton OH 45440-3638

michael.brown@wpafb.af.mil

Sivaram P. Gogineni
Innovative Scientific Solutions, Inc.
Dayton OH 45440-3638

sivaram.gogineni@wpafb.af.mil

ABSTRACT

While optical diagnostic techniques have been applied with great success to the fundamental study of combustion chemistry and physics in the laboratory, the challenges afforded by real-world propulsion systems demand continuing innovation if such techniques are to be adapted and transitioned for use in engineering tests and on-board monitoring and control applications. This paper documents continuing efforts to transition aerodynamic measurement technologies from diagnostics-development laboratories to combustor test-and-evaluation facilities in the Propulsion Directorate's Combustion Branch (Turbine Engine Division). Applications of various optical diagnostic techniques for visualizing flowfields and quantifying temperatures and key species concentrations in several advanced combustors are described.

1.0 INTRODUCTION

Propulsion systems represent a substantial fraction of the cost, weight, and complexity of Air Force aircraft, spacecraft, and other weapon-system platforms. The vast majority of these propulsion systems are powered through combustion of fuel; therefore, the detailed study of combustion has emerged as a highly relevant and important field of endeavor. Much of the work performed by today's combustion scientists and engineers is devoted to the tasks of improving propulsion-system performance while simultaneously reducing pollutant emissions. Increasing the affordability, maintainability, and reliability of these systems is also a major driver.

While improved performance can be described quantitatively in many terms (*e.g.*, specific fuel consumption, thrust-to-weight ratio, etc.), it often involves efforts to increase heat release during the combustion process. Improvements may be achieved as well by reducing the length and/or weight of the combustor through informed design decisions. Engine emissions that might adversely impact the environment and the military signature of Air Force systems must be reduced while striving to improve performance. Judicious design and control of the combustor can significantly impact the affordability, maintainability, and reliability of the propulsion system by extending the useful life of engine components or by permitting the incorporation of less-expensive materials in combustor construction, for example. Pursuing these goals requires a thorough understanding of the fundamental physics and chemistry of combustion processes.

The Combustion Branch of the Air Force Research Laboratory's Propulsion Directorate (Turbine Engine Division) has adopted a philosophy for combustor-technology development aimed at achieving these goals. At the basic-research level, new diagnostic approaches are developed and tested in conjunction with extensive modeling-and-simulation efforts. Techniques are "cross-validated" through studies of fundamental combustion processes in laboratory rigs that provide favorable optical conditions while remaining computationally tractable. Axisymmetric burners with ample optical access and well-defined boundary conditions represent such test articles. The measurement and computational tools designed, tested, and matured through this basic research are applied subsequently to hardware testing and evaluation. Ultimately, sensor platforms based on these diagnostic approaches and algorithms derived in part from the combustion models are incorporated for on-board propulsion-system monitoring and control.

Development, demonstration, and application of laser-based and other optical diagnostic techniques are integral elements of that research plan. Advanced measurement techniques that exploit lasers and optics have become well-established tools for characterizing combustion.[1] Non-invasive measurement approaches are often ideally suited for visualizing complex reacting flowfields and quantifying key chemical-species concentrations and fluid-dynamic parameters. The fundamental information these techniques provide is essential for achieving a detailed understanding of the chemistry and physics of combustion processes. Furthermore, these data are critical for validating combustion models and combustor-design codes with tremendous potential for propulsion-system development. At a more applied level, hardened diagnostics provide the designer with performance data for the systems-engineering process. Diagnostics also promise to play an important role in fielded propulsion systems as elements in control and optimization schemes.

These characteristics of optical diagnostic techniques suggest a three-phased evolutionary process for their development and application. In the first phase, emphasis is placed on the diagnostic technique itself—on the chemistry and physics that define the measurement and the hardware (sources, optics, detectors, etc.) and software necessary to accomplish that measurement. During this phase of the process, a research-grade instrument is typically employed to study a well-characterized flowfield in a laboratory environment. While this phase of the diagnostics-development process is certainly essential and exciting, the ultimate utility of a diagnostic technique is significantly limited if it never sees application beyond the laboratory.

During the second phase of the process, a hardened version of the research-grade instrument is applied to achieving measurements in an engineering facility. The emphasis in this phase shifts from the diagnostic technique to the engineering application. In the third phase, a miniaturized and robust diagnostic device is incorporated into the final product, such as an actual gas turbine engine, for on-board sensing and control.

The transitions from laboratory to facility to fielded systems are fraught with significant challenges that must be addressed. During the laboratory phase of diagnostics development, conditions are typically ideal and well controlled. They might involve vibrationally isolated laser tables, humidity- and temperature-controlled environments, and sufficient space to accommodate sources, optics, mounts, and detectors required to achieve the desired measurement. Test articles often feature ample optical access and support clean-burning, gas-fueled, laminar flames operating under atmospheric or sub-atmospheric conditions. In contrast, facilities applications involve conditions characteristic of actual engine hardware. Challenges include extreme environmental conditions (heat, vibration, acoustics, etc.), limited optical access, tight geometric constraints, little operational space, fully developed turbulence, two-phase flows, soot formation, high pressure, collisional quenching, energy redistribution, optical thickness, beam steering, high background luminosity, and scattering and spectral interferences. These challenges are amplified on moving from the facility to the on-board environment. Successful transitions, first from the laboratory to the facility and then from the facility to the field, require thoughtful attention to these issues.

This paper continues with descriptions of three specific scenarios in which optical diagnostics have been applied to assess the performance and impact the design of next-generation combustors and fuels through ground testing. These applications and other opportunities for ground-test and on-board applications will be discussed in the briefing that accompanies this paper.

2.0 FLOW VISUALIZATION IN THE TRAPPED-VORTEX COMBUSTOR (TVC)

Experimental and computational techniques for the visualization of fluid flows have emerged as essential tools for increasing our understanding of the physics and chemistry of these flows. Indeed, many—if not most—of the breakthroughs in fluid mechanics and dynamics can be attributed to the understanding achieved through imaging of the various multidimensional structures in fluid flow. High-speed digital imaging, planar laser-induced fluorescence (PLIF), particle-image velocimetry (PIV), coherent-structure velocimetry (CSV), and laser-induced incandescence (LII) are amongst the diagnostic tools routinely employed for two-dimensional flow visualization in the test facilities of the Combustion Branch.

The unique geometry of the TVC has been designed to bring improved overall performance, enhanced stability, and reduced pollutant emissions to current and next-generation propulsion systems.[2,3] It also promises benefits in terms of combustor length and pressure drop. The key features of the TVC design are evident in Fig. 1, which depicts a natural-gas-fueled TVC sector operating at atmospheric pressure. Cavities at the top and bottom of the sector promote aerodynamic trapping of a combusting vortex. Injection of fuel and air into these cavities maintains continuous pilot flames therein, enhancing fuel-air mixing and flame stability. These trapped pilot flames interact with the main fuel/air flow situated between the two cavities.

Ongoing testing of various TVC sectors is aimed at establishing design rules and assessing the performance impacts of such drivers as cavity and main geometry, fuel-injector design and placement, and air flow. Enhanced mixing techniques aimed at reducing pollutant emissions and combustor size are also under study. These efforts are supported by flow visualization achieved through high-speed digital imaging, PLIF, PIV, and CSV.

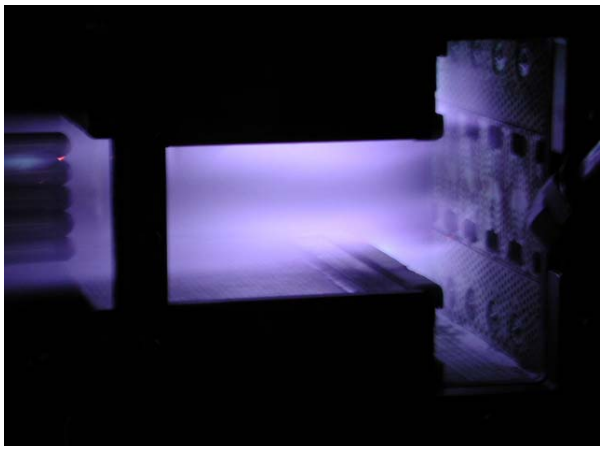

Figure 1. Natural-gas-fueled TVC sector operating at atmospheric pressure. Flow is from right to left.

High-speed digital images of the TVC have been acquired using a Phantom v5.0 CMOS-based high-framing-rate digital camera provided by Photo-Sonics International Ltd. During this study, the camera was operated at 11,200 frames per second (fps) with a resolution of 256×256 pixels and an exposure time of 10 μs. Frame captures of the normalized flame luminosity in a JP-8-fueled TVC sector operating at pressures of 8.5 and 12 atm are depicted in Fig. 2. These high-speed visualizations provide real-time feedback during TVC testing regarding the flow pattern and flame distribution within the cavities and main sections of the combustors. Exposure times as low as 10 μs enable flow freezing not achievable through conventional videography.

When viewed in a time-correlated sequence, such images clearly show vortical flame structures in the upper and lower cavities. These vortices act as flame holders that promote flame stability and enhance fuel-air mixing by increasing the turbulence level and the residence time.

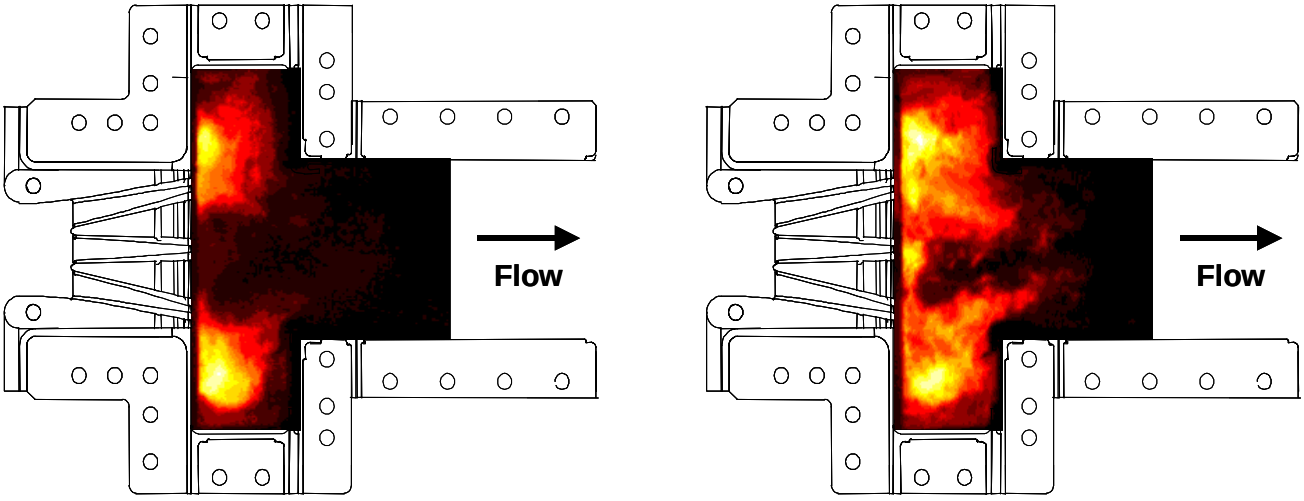

Figure 2. Flame luminosity captured with a high-speed digital camera from a JP-8-fueled TVC sector operating at 8.5 atm (left) and 12 atm (right).

While high-speed digital imaging provides a qualitative description of flame location and dynamics, PLIF can be used to visualize specific flame species. This yields a more accurate measurement of flame location and eliminates the spatial ambiguity associated with line-of-sight averaging. In the current work, PLIF of the hydroxyl radical (OH) was accomplished by exciting the $R_1(8)$ transition of the (1,0) band in the A-X system. The requisite 281.3414-nm laser sheet was generated using the frequency-doubled output of a Nd:YAG-pumped dye laser, and fluorescence from the A-X (1,1) and (0,0) bands was detected using an intensified charge-coupled device (ICCD) camera equipped with a UG-11 and two WG-295 colored glass filters to reduce visible and laser-scattered light, respectively.

OH-PLIF images were acquired in a natural-gas-fueled TVC sector for a number of fuel-injection configurations. Injection in the cavity and main sections produces the flame pattern in Fig. 3. The flame pattern obtained in the lower cavity through fuel injection in the cavity alone is depicted in Fig. 4. These data are employed to verify calculations using a conventional k-ε-based CFD code with chemistry.

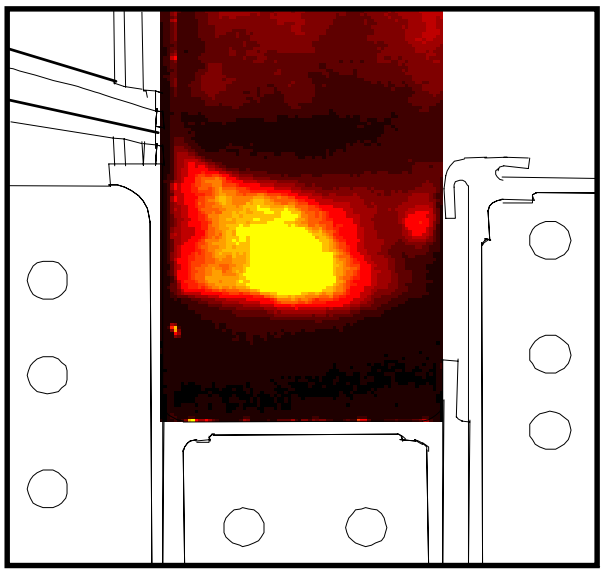

Figure 3. OH-PLIF signal obtained in the lower cavity of a natural-gas-fueled TVC with fuel injection in the cavity and main sections.

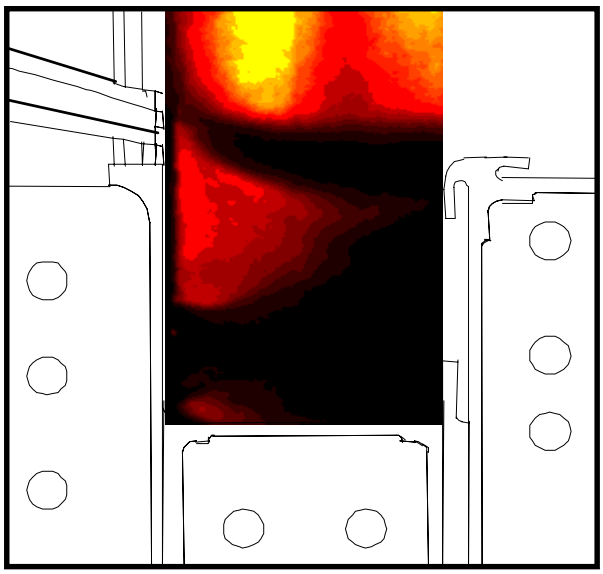

Figure 4. OH-PLIF signal obtained in the lower cavity of a natural-gas-fueled TVC with fuel injection in the cavity alone.

Velocimetry data have been acquired to complement these flame visualizations. PIV was achieved using a dual-image, digital cross-correlation configuration with two Nd:YAG lasers and a dual-frame Kodak ES4 2000×2000 pixel CCD camera. Vectors were computed using a dPIV code developed by AFRL and Innovative Scientific Solutions, Inc., using 16×16 pixel interrogation regions and 75% overlap. An average of five image pairs was employed to generate the data in Fig. 5, which compare the velocities determined by PIV in the lower cavity of the TVC sector with those computed using a commercial CFD package.

The short-exposure images acquired with the high-speed digital camera can also be used to estimate flow velocities subject to certain assumptions using CSV. This involves several image-processing steps, including the generation of isoline contours to define structure boundaries, the selection of an optimal interrogation window and overlap parameter, and cross-correlation between image pairs for determination of the local

displacement vectors. It must be stressed that CSV in combusting flows cannot provide a true measure of convective velocity due to inherent non-convective flame-intensity variations. Nonetheless, slowly varying flame structures can provide a qualitative picture of the flow structure. Such a technique can be highly valuable for flow analysis on-demand and can supplement more difficult, laser-based methods such as PIV. The latter is valuable for quantitative velocimetry and code validation, but it is not conducive to continuous operation due to window fouling and seed build-up in small passages.

The CSV image in Fig. 6 depicts the combusting flow pattern with a cavity geometry very similar to that in which the PIV data of Fig. 5 were acquired. Qualitative agreement between the two velocity fields is quite good.

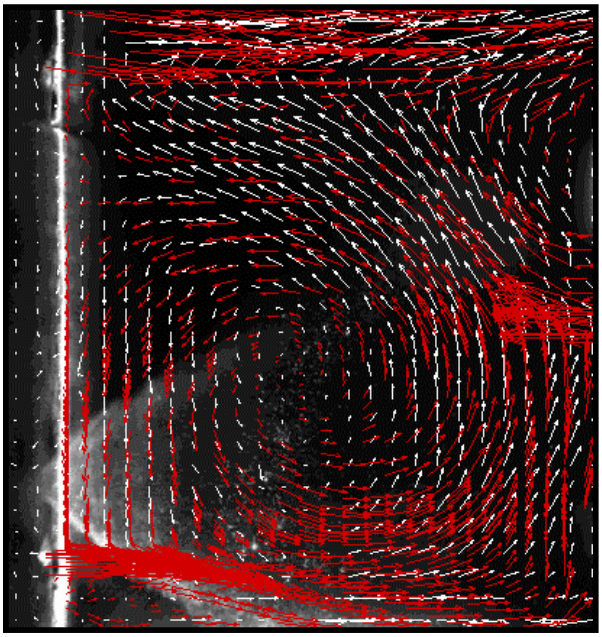

Figure 5. Comparison of PIV data (white vectors) and CFD data (red vectors) acquired in the lower cavity of a TVC sector under non-combusting

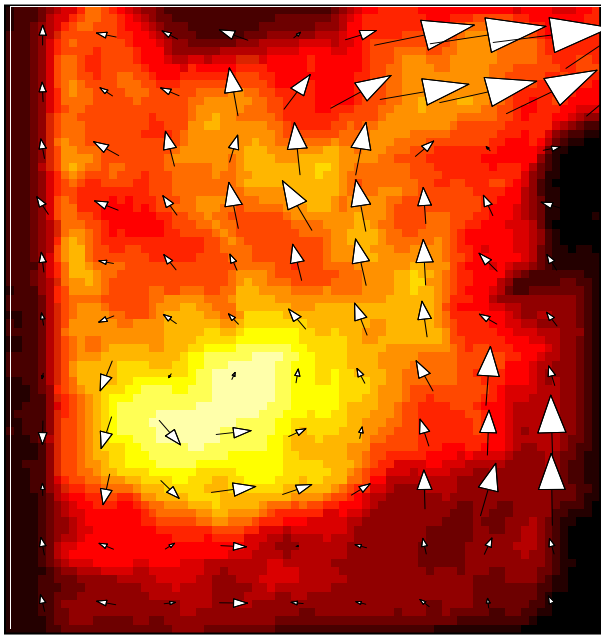

Figure 6. CSV data overlayed on a high-speed digital image of combustion in the lower cavity of a TVC sector.

3.0 SIMULTANEOUS PLANAR LII, OH PLIF, AND DROPLET MIE SCATTERING IN A CFM56-BASED MODEL COMBUSTOR

Swirl-stabilized liquid-spray injectors are commonly used in gas-turbine engines to achieve compact, stable, and efficient combustion. The flowfield in the primary zone of such a spray flame is characterized by high shear stresses and turbulent intensities that result in vortex breakdown and large-scale unsteady motions.[4,5] These unsteady motions are known to play a key role in the formation of pollutant emissions such as carbon monoxide (CO), nitric oxide (NO), and unburned hydrocarbons (UHC).[6-8] Considerably less is known, however, about the mechanisms that lead to soot formation in swirl-stabilized, liquid-fueled combustors. Previous investigations have relied on exhaust-gas measurements and parametric studies to gain insight into

the effects of various input conditions on soot loading.[9-12] Much of the fundamental knowledge concerning soot formation is derived from investigations of laminar diffusion flames,[13-15] with only a limited number of studies having focused on unsteady effects.[16,17] The importance of considering unsteadiness and fluid-flame interactions was demonstrated by Shaddix et al.,[17] who found that a forced methane/air diffusion flame produced a four-fold increase in soot volume fraction (as a result of increased particle size) as compared with a steady flame having the same mean fuel-flow velocity.

The goal of the current investigation is to study soot formation in the highly dynamic environment of a swirl-stabilized, liquid-fueled combustor. This is accomplished using simultaneous imaging of the soot volume fraction, hydroxyl-radical (OH) distribution, and droplet pattern in the primary reaction zone using laser-induced incandescence (LII), OH planar laser-induced fluorescence (PLIF), and droplet Mie scattering, respectively. The utility of LII for two-dimensional imaging of soot volume fraction has been demonstrated in laboratory investigations[18,19] as well as in aircraft engine exhausts.[12,13] Brown et al.[20] performed planar LII for soot-volume-fraction imaging in the reaction zone of a gas-turbine combustor; their preliminary measurements employed LII alone for demonstration purposes and did not image the turbulent flame structure near the exit of the swirl cup. In the current work, we extend the work of Brown et al.[20] by performing LII at the exit of the swirl cup and by adding OH PLIF and Mie scattering diagnostics.

The use of OH as a flame marker is typical in studies of soot formation in diffusion flames because of its close correlation with flame temperature.[21,22] It has also been employed in a number of investigations of swirl-stabilized combustors.[23,24] The use of laser-saturated OH LIF for *quantitative* measurements has also been demonstrated,[25,26] although saturation is quite difficult in the case of planar measurements. In the current investigation, we demonstrate qualitative measurements in the recirculation region using excitation levels well below saturation. OH-PLIF measurements in the liquid-spray region are more uncertain because of simultaneous droplet scattering and non-equilibrium conditions, although meaningful measurements are possible with careful consideration of potential errors. Mie scattering from large droplets, which appears in the OH images but does not preclude signal interpretation, is used to a limited extent as a spray diagnostic. As shown in Fig. 7, the experimental set-up includes an Nd:YAG for saturated LII at 532 nm and a narrowband dye laser for OH PLIF using the $Q_1(9)$ line in the 1-0 band of the A-X system.

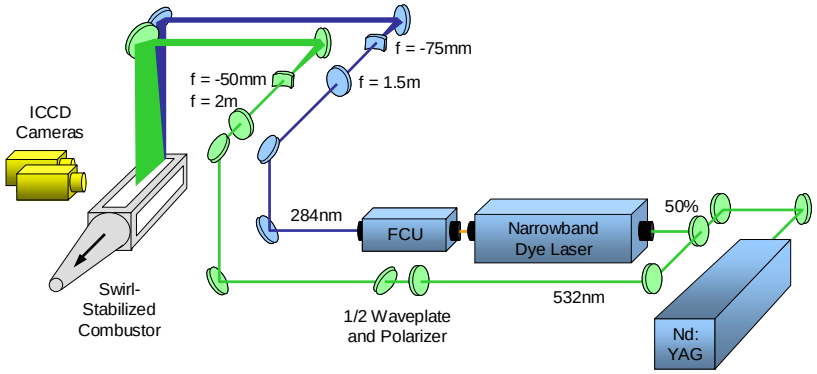

Figure. 7. Simultaneous OH PLIF and LII in atmospheric-pressure, swirl-stabilized, JP8-fueled, model gas-turbine combustor.

The injector geometry and sample instantaneous OH-PLIF images for JP-8 and a non-aromatic liquid fuel are shown in Fig. 8 at an equivalence ratio of 0.8. Such images provide a clear indication of the intermittency

within the primary flame zone and are useful for characterizing the statistical behavior in terms of probability density functions. It is found, for example, that large-scale structures play a key role in the soot formation process. Intermittent regions of rich premixed fuel and air develop between the primary flame layer and recirculation zone that serve as sites for soot inception. The rate of soot production is dependent upon the frequency and spatial extent of these regions, while the rate of soot oxidation is dependent upon the availability of oxygen and OH in the primary zone and recirculation region. Hence, the overall soot volume fraction is highly sensitive to the dynamics of the injection process as well as to the local, unsteady equivalence ratio. The importance of the former is highlighted by differences in the vaporization and soot formation characteristics of JP-8 versus non-aromatic fuels, as shown in Figs. 8(b) and 2(c).

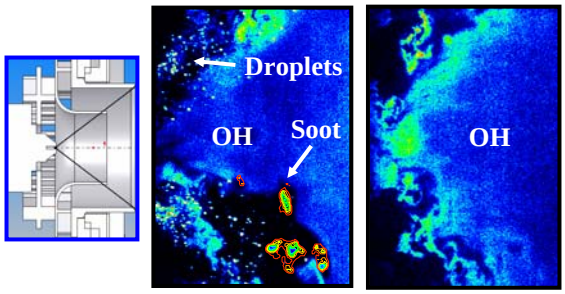

Figure 8. (a) Dual-radial swirl cup with center-mounted pressure-swirl injector, (b) primary zone with JP-8 at ϕ = 0.8, and (c) primary zone with non-aromatic fuel at ϕ = 0.8.

In studies of soot-mitigating additives, performed in collaboration with the Fuels Branch of ARFL, the simultaneous OH-PLIF and LII measurements were used to determine whether changes in soot production result from changes in the chemical or physical properties of the fuel. Figures 9(a) and 9(b) demonstrate the ability of the current measurement system to track local equivalence ratio and soot production, respectively. Using a droplet-free region in the recirculation zone, the time- and spatially averaged OH-PLIF signal is plotted with respect to equivalence ratio and compared with an equilibrium calculation. This provides a calibration for JP-8 that can be used qualitatively to track changes in equivalence ratio. The data in Fig. 9(a) include corrections for the effects of collisional quenching and Boltzmann-fraction variations on the OH-PLIF signal. The LII data in Fig. 9(b) show an exponential increase of the soot volume fraction in the primary zone with respect to equivalence ratio. A subsequent test using an increased LII-gate period demonstrates minimal particle-size bias and measurement repeatability. Note that the exhaust-gas sampling probe displays a threshold effect at about ϕ = 1.0 below which soot in the exhaust is effectively oxidized by OH and O_2 due to long residence times.

Since the dependence of soot on equivalence ratio is exponential, slight changes in equivalence ratio could easily be mistaken for changes in soot particle counts in the exhaust stream. This highlights the importance of tracking equivalence ratio while performing studies of soot-mitigating additives. An example is shown in Fig. 10 where methyl acetate is added to the fuel during a test. Note the large decrease in soot volume fraction during methyl-acetate addition, as measured by LII; this corresponds to a large decrease in particle counts from the sampling probe. Note also the increase in OH-PLIF signal that, according to the results of Fig. 9(a), indicates that the fuel mixture is becoming leaner. A certain ambiguity exists, however, because the final equivalence ratio could lie on either side of the peak OH signal. Using the exponential fit to the data in Fig. 9(b), however, the change in LII signal corresponds to an equivalence ratio that is slightly on the rich side of

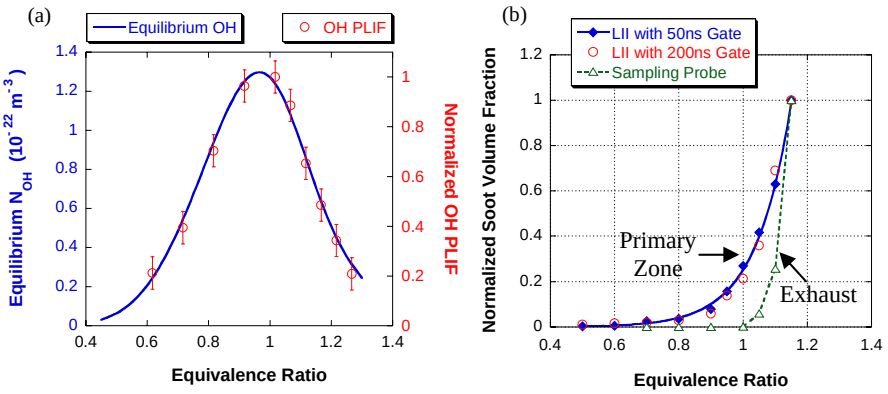

Figure 9. (a) Fit of OH data in recirculation region with equilibrium calculations and (b) comparison of normalized soot volume fraction in primary zone with particle counts in the exhaust stream.

the OH peak. An overall equivalence-ratio decrease of 0.123 due to methyl-acetate addition is measured to within 1% for both the OH-PLIF and LII data and to within 10% of flow calculations. The agreement between OH-PLIF and LII data indicates that methyl acetate in the current study did not have an effect on soot production, except for its effect on equivalence ratio. One can envision, therefore, the use of a combined LIF and LII system to track the performance of soot-mitigating additives without uncertainties in equivalence ratio.

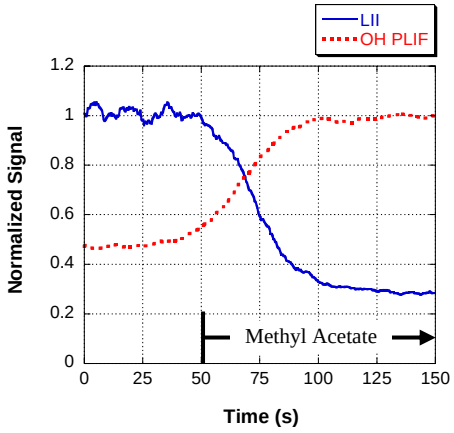

Figure 10. Drop in soot due to methyl acetate addition corresponds to decrease in ϕ as verified by OH PLIF.

4.0 TRANSIENT-GRATING THERMOMETRY IN THE TVC

Laser-induced transient or dynamic gratings have an established diagnostic history for measurement of a wide range of physical properties, including fast-carrier lifetimes, diffusion rates, and temperature. Transient-grating spectroscopy (TGS) has been repeatedly demonstrated as a technique that is suitable for application in

hydrocarbon-air flames.[27,28] In particular, single-shot thermometry has been demonstrated under various combustion conditions.[28] The coherent signal is generated by Bragg scattering a continuous-wave probe beam from a laser-induced refractive-index grating that is established through the spatial and temporal overlap of two pump beams derived from the same pulsed laser.[29] The index grating is established through electrostriction or optical absorption and subsequent molecular collisions that transfer the absorbed energy to translational motion. The time-resolved signal appears as a damped sinusoidal oscillation. The oscillation frequency is determined by the grating spacing and the local speed of sound, which, in turn, is a function of temperature. Extraction of the temperature from the measured sound speed requires some knowledge of the ratio of the molecular mass to the specific heat ratio. For hydrocarbon-air combustion, this ratio is a very weak function of the exact mixture fraction and temperature.[28] Consequently, a reasonable estimate of the value of the ratio leads to accurate temperature measurements, which are easily accomplished and render the technique applicable under a wide range of combustion conditions.

Execution of the transient-grating technique requires three incident beams from two laser sources—a pulsed pump laser and a continuous-wave probe laser. The output of the pump laser is split into two beams of equal intensity that are crossed at a small angle. The spatial and temporal overlap of the pump beams creates an optical-intensity pattern that couples a very small amount of energy via electrostriction or absorption into the test region, thereby modifying the local index of refraction. The probe laser beam—incident at the Bragg scattering angle—is reflected by the spatially modulated index grating and detects the time evolution of the grating. (A schematic of the incident-beam arrangement is shown in Figure 11.) The grating structure in the fluid returns to local equilibrium through acoustic and thermal modes. The counter-propagating acoustic modes alternately interfere constructively and destructively. This imposes a temporal modulation on the signal, the period of which is determined by the local speed of sound and the grating spacing. Since the speed of sound is a function of temperature, the technique provides thermometry with high spatial resolution.

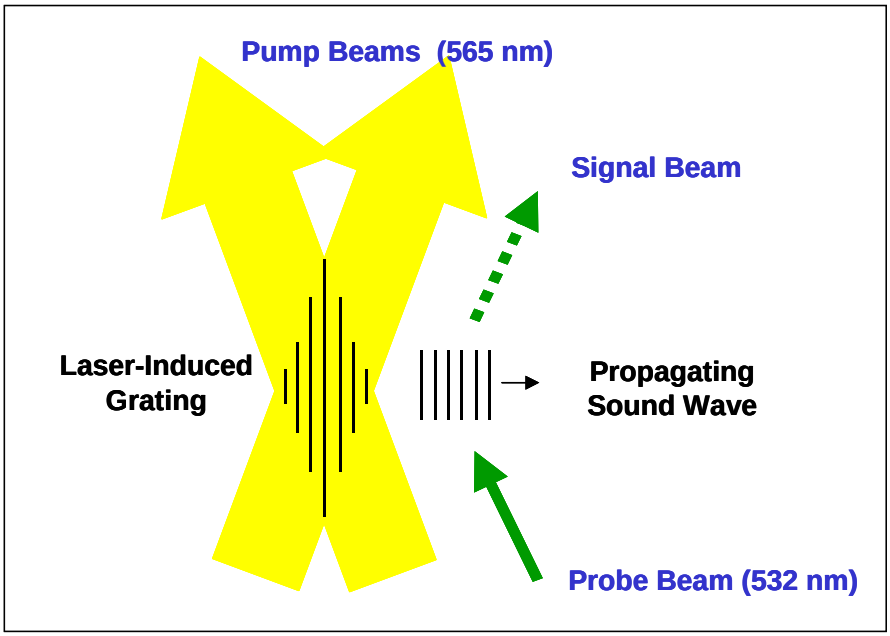

Figure 11. Schematic of incident-beam arrangement for TVC measurements. Note probe and signal beams were slightly out-of-plane with respect to pump beams.

As part of our continuing effort to develop and apply this technique, transient grating thermometry has been performed in the rich flame zone of a TVC operating under turbulent, pressurized, JP-8-fueled conditions. Measurements were accomplished at pressures of 50, 75, and 100 psi with local equivalence ratios in the range 1–1.25. The pump beams were derived from the 565-nm output of a Nd:YAG-pumped dye laser. The cw output of a vanadate laser (532 nm) provided the probe beam. While the pump lasers were not tuned to a particular molecular resonance, the detected signals showed clear signs of thermalization and the absence of nonresonant electrostriction. Soot particles and soot precursors are the likely absorbers responsible for signal generation. Beam steering was clearly evident in the form of variable pointing and random spatial modulation of the exiting beams. Due to such adverse affects, signal was not obtained on all laser shots; however, useful signals were generated with sufficient frequency to permit meaningful temperature measurements.

A typical single-shot signal is depicted in Fig. 12. Four oscillations are clearly seen. (We have found in practice that only three rings are needed for precise temperature determination.) The power spectrum corresponding to this signal is shown in Fig. 13. It is dominated by two features: a) the Rayleigh peak centered at zero frequency associated with the non-propagating thermal mode and b) the Brillouin feature associated with the counter-propagating acoustic modes. Temperature is extracted from each analyzed single-shot signal through numerical determination of the peak of the Brillouin feature in the power spectrum.

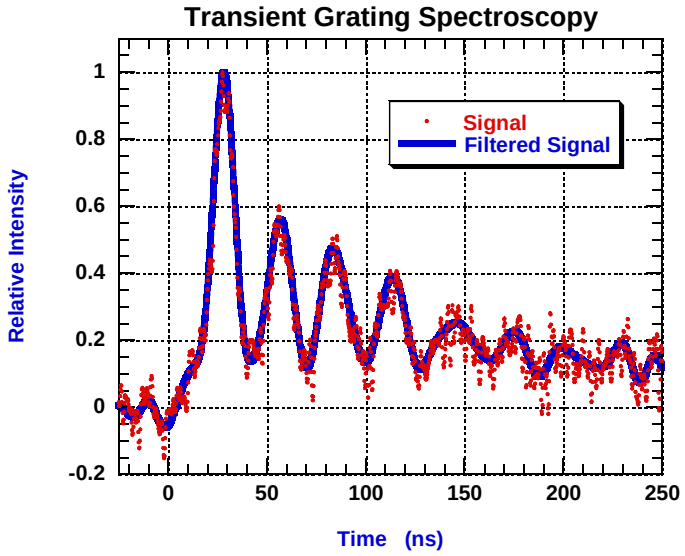

Figure 12. Single-shot TGS signal acquired in the rich flame zone of a TVC operating under turbulent, pressurized (75 psi), JP-8-fueled conditions.

In one particular data-collection run, the TVC was operated with the cavity slightly rich (equivalence ratio of ~ 1.1) at 100 psi. Signal from 1300 sequential laser shots was recorded at this condition. Roughly one-third of the single-shot signals were found to be legitimate analyzable TGS signals; the remainder were found to be compromised by electronic noise (low S/N) or beam steering. Down-selection of signals to be analyzed was performed in a two-step process. Each time-domain signal was first examined to ensure that the peak signal location fell within a meaningful delay with respect to the arrival of the pump beams. (The delay is associated with the dynamics of the grating formation.) After zero padding, each power spectrum was constructed using standard FFT routines, and the ratio of the amplitude of the Brillouin peak to that of the Rayleigh peak was

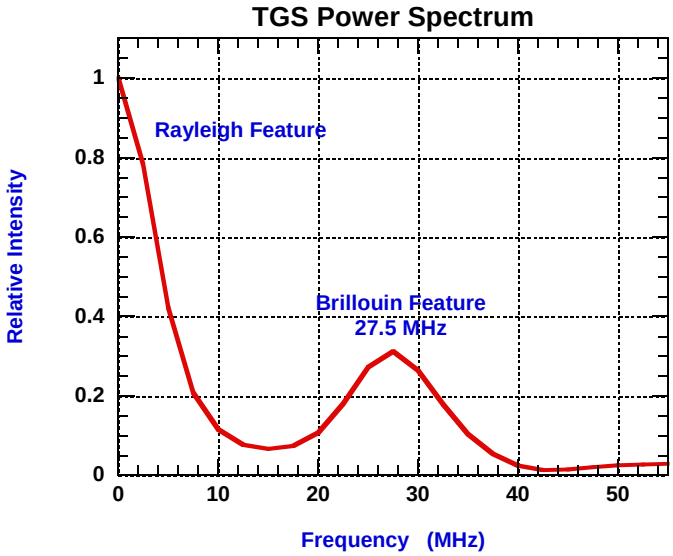

Figure 13. Power spectrum of signal shown in Fig. 12.

then determined. Spectra that exhibited ratios >0.005 were then analyzed in detail. The Brillouin feature of the down-selected set of 456 power spectra was fit using a fourth-order polynomial to find the peak. The corresponding temperatures are presented as a histogram in Fig. 14. The mean value of the temperature is 2260 K and is quite comparable to the adiabatic-flame-temperature values for decane and dodecane (sometimes considered to be single-component surrogates for JP-8) of 2200 and 2300 K, respectively. The breadth of the histogram largely reflects the local dynamic nature of the reaction zone as pockets of fluid in different relative states of combustion maturity pass through the probe volume.

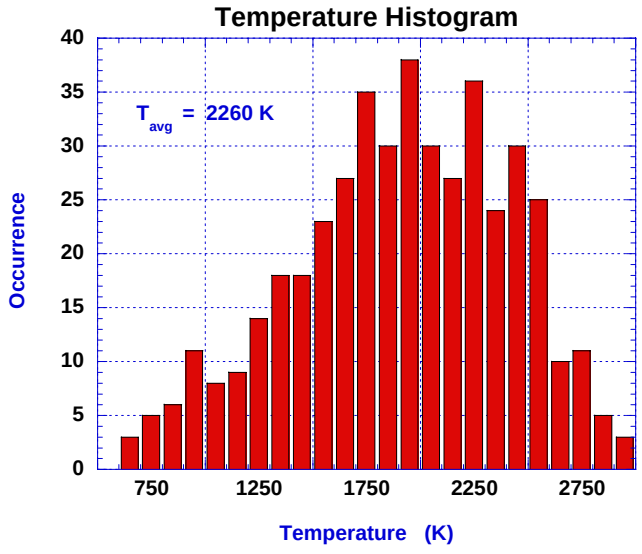

Figure 14. Temperature histogram constructed through analysis of 456 single-shot signals acquired in a TVC operating at a pressure of 100 psi.

The width of the Rayleigh feature is determined by the local thermal diffusivity and the width of the Brillouin feature is proportional to the acoustic damping coefficient that has contributions from thermal and mass diffusion, sheer and bulk viscosity. The width of these features is easily determined via fitting with power spectral functions found in the literature, permitting extraction of values for the thermal diffusivity and acoustic damping coefficient. For power spectra that exhibit temperatures near the peak of the temperature histogram (~2200 ± 300 K), the extracted thermal diffusivity is found to vary by ~18% shot-to-shot while the acoustic damping coefficient varies by ~70%. Both the measured thermal diffusivity and acoustic damping coefficient are larger than the corresponding values calculated using the output of an equilibrium flame code that accounts only for the gas species present and not for soot. The difference between the measured and calculated values probably reflects the soot loading in the rich reaction zone.[30] Our current efforts are aimed at quantifying the contribution of soot to these transport properties.

5.0 CONCLUSION

Tremendous time and energy have been invested throughout the research community in the development of advanced optical diagnostics for the fundamental study of combustion chemistry and physics. The techniques developed for these important basic-research activities also have enormous potential for impacting the design, development, test, evaluation, operation, and maintenance of current and next-generation propulsion systems when those techniques are transitioned from the laboratory to the test facility and ultimately to the field.

This paper summarizes some recent efforts to transition diagnostics for use in the combustor-test facilities of the Combustion Branch at Wright-Patterson Air Force Base. Various techniques for flow visualization, including high-speed digital imaging, PLIF, PIV, CSV, and LII, as well as methods for measuring temperatures, species, and equivalence ratio have been applied in these facilities.

6.0 ACKNOWLEDGMENTS

The authors gratefully acknowledge myriad technical contributions from the members of the Combustion Branch of the Air Force Research Laboratory's Propulsion Directorate (Turbine Engine Division) and the contractors supporting that branch, especially Innovative Scientific Solutions, Inc. Financial support from the Air Force Office of Scientific Research (Dr. Julian Tishkoff, Program Manager) is gratefully acknowledged as well.

7.0 REFERENCES

[1] A. C. Eckbreth, *Laser Diagnostics for Combustion, Temperature, and Species*, 2nd Edition, Gordon & Breach, 1996.

[2] W. M. Roquemore, D. Shouse, D. Burrus, A. Johnson, C. Cooper, B. Duncan, K.-Y. Hsu, V. R. Katta, G. J. Sturgess, and I. Vihinen, "Trapped Vortex Combustor Concept for Gas Turbine Engines," AIAA 2001-0483 (2001).

[3] T. R. Meyer, M. S. Brown, S. Fonov, L. P. Goss, J. R. Gord, D. T. Shouse, V. M. Belovich, W. M. Roquemore, C. S. Cooper, E. S. Kim, and J. Haynes, "Optical Diagnostics and Numerical Characterization of a Trapped-Vortex Combustor," AIAA 2002-3863 (2002).

[4] W.-W. Kim, S. Menon, and H. Mongia, "Large-Eddy Simulation of a Gas Turbine Combustor Flow," Combust. Sci. Technol. **143**, 25-62 (1999).

[5] S. Wang, S.-Y. Hsieh, and V. Yang, "Numerical Simulation of Gas Turbine Swirl-Stabilized Injector Dynamics," AIAA 2001-0334 (2001).

[6] M. V. Heitor and J. H. Whitelaw, "Velocity, Temperature, and Species Characteristics of the Flow in a Gas-Turbine Combustor," Combust. Flame **64**, 1-32 (1986).

[7] A. F. Bicen, D. G. N. Tse, and J. H. Whitelaw, "Combustion Characteristics of a Model Can-Type Combustor," Combust. Flame **80**, 111-125 (1990).

[8] T. J. Held, M. A. Mueller, S.-C. Li, and H. Mongia, "Data-Driven Model for NO_x, CO and UHC Emissions for a Dry Low Emissions Gas Turbine Combustor," AIAA 2001-3425 ((2001).

[9] W. A. Eckerle, "Soot Loading in a Generic Gas Turbine Combustor," AIAA 87-0297 (1987).

[10] T. C. Fang, C. M. Megaridis, W. A. Sowa, and G. S. Samuelsen, "Soot Morphology in a Liquid-Fueled Swirl-Stabilized Combustor," Combust. Flame **112**, 312-328 (1998).

[11] J. D. Black, "Laser Induced Incandescence Measurements of Particles in Aero-Engine Exhausts," SPIE Vol. 3821, EUROPTO Conference on Environmental Sensing and Applications, Munich, Germany (1999).

[12] D. R. Snelling, K. A. Thomson, G. J. Smallwood, and O. L. Gulder, "Two-Dimensional Imaging of Soot Volume Fraction in Laminar Diffusion Flames," Appl. Opt. **38**, 2478-1485 (1999).

[13] T. P. Jenkins, J. L. Bartholomew, P. A. DeBarber, P. Yang, J. M. Seitzman, and R. P. Howard, "A Laser-Induced Incandescence System for Measuring Soot Flux in Aircraft Engine Exhausts," AIAA 2002-3736 (2002).

[14] R. J. Santoro, T. T. Yeh, J. J. Horvath, and H. G. Semerjian, "The Transport and Growth of Soot Particles in Laminar Diffusion Flames," Combust. Sci. Technol. **53**, 89-115 (1987).

[15] D. L. Urban and G. M. Faeth, "Soot Research in Combustion Science: Introduction and Review of Current Work," AIAA 2001-0322 (2001).

[16] Y.-H. Won, T. Kamimoto, H. Kobayashi, and H. Kosaka, "2-D Soot Visualization in Unsteady Spray Flame by Means of Laser Sheet Scattering Technique," SAE Tech. Paper 910223 (1991).

[17] C. R. Shaddix, J. E. Harrington, and K. C. Smyth, "Quantitative Measurements of Enhanced Soot Production in a Flickering Methane / Air Diffusion Flame," Combust. Flame **99**, 723-732 (1994).

[18] B. Quay, T.-W. Lee, T. Ni, and R. J. Santoro, "Spatially Resolved Measurements of Soot Volume Fraction Using Laser-Induced Incandescence," Combust. Flame **97**, 384-392 (1994).

[19] R. L. Vander Wal and K. J. Weiland, "Laser-Induced Incandescence: Development and Characterization Towards a Measurement of Soot-Volume Fraction," Appl. Phys. B **59**, 445-452 (1994).

[20] M. S. Brown, T. R. Meyer, J. R. Gord, V. M. Belovich, and W. M. Roquemore, "Laser-Induced Incandescence Measurements in the Reaction Zone of a Model Gas Turbine Combustor," AIAA 2002-0393 (2002).

[21] K. C. Smyth, J. H. Miller, R. C. Dorfman, W. G. Mallard, and R. J. Santoro, "Soot Inception in a Methane/Air Diffusion Flame as Characterized by Detailed Species Profiles," Combust. Flame **62**, 157-181 (1985).

[22] F. Cignoli, S. Benecchi, and Z. Giorgio, "Simultaneous One-Dimensional Visualization of OH, Polycyclic Aromatic Hydrocarbons, and Soot, in a Laminar Diffusion Flame," Opt. Lett. **17**, 229-231 (1992).

[23] W.-P. Shih, J. G. Lee, and D. A. Santavicca, "Stability and Emissions Characteristics of a Lean Premixed Gas Turbine Combustor," in the Twenty-Sixth Symposium (International) on Combustion (The Combustion Institute, Pittsburg, PA, 1996).

[24] R. E. Foglesong, T. R. Frazier, L. M. Flamand, J. E. Peters, and R. P. Lucht, "Flame Structure and Emissions Characteristics of a Lean Premixed Gas Turbine Combustor," AIAA 99-2399 (1999).

[25] R. P. Lucht, D. W. Sweeney, and N. M. Laurendeau, "Laser-Saturated Fluorescence Measurements of OH Concentration in Flames," Combust. Flame **50**, 189-205 (1983).

[26] C. D. Carter, G. B. King, and N. M. Laurendeau, "Saturated Fluorescence Measurements of the Hydroxyl Radical in Laminar High-Pressure $C_2H_6/O_2/N_2$ Flames," Appl. Opt. **31**, 1511-1522 (1992).

[27] M.S. Brown and W.L. Roberts, "Single-Point Thermometry in High Pressure, Sooting, Combustion Environments," J. Prop. Power **15**, 119-127 (1999).

[28] M. S. Brown, Y. Li, W. Roberts, and J. R. Gord, "Analysis of Transient-Grating Signals for Reacting-Flow Applications," Appl. Opt. **42**, 566-578 (2003).

[29] H. J. Eichler, P. Gunter, and D. W. Pohl, *Laser-Induced Dynamic Gratings*, Springer-Verlag, 1986.

[30] N.E. Molevich and V.E. Nenashev, "Effect of the Bulk Viscosity on the Sound Propagation in Nonequilibrium Suspensions of Microparticles in Gas," Acoust. Phys. **46**, 450-455 (2000).